Fluorinated phosphonate analogues of phenylalanine: Synthesis, X-ray and DFT studies

Joanna Kwiczak-Yiğitbaşi, Jean-Luc Pirat, David Virieux, Jean-Noël Null Volle, Agnieszka Janiak, Marcin Hoffmann, Donata Pluskota-Karwatka

Arabian Journal of Chemistry (2020) 13, 2384–2399

King Saud University

Arabian Journal of Chemistry

www.ksu.edu.sa
www.sciencedirect.com

ORIGINAL ARTICLE

Fluorinated phosphonate analogues of phenylalanine: Synthesis, X-ray and DFT studies

Joanna Kwiczak-Yiğitbaşı [a,b], Jean-Luc Pirat [b], David Virieux [b], Jean-Noël Volle [b,*], Agnieszka Janiak [a], Marcin Hoffmann [a], Donata Pluskota-Karwatka [a,*]

[a] *Adam Mickiewicz University in Poznań, Faculty of Chemistry, Umultowska 89b, 61-614 Poznań, Poland*
[b] *AM2N, UMR 5253, ICGM, ENSCM, 8 rue de l'Ecole Normale, 34296 Montpellier Cedex 5, France*

Received 12 December 2017; accepted 6 May 2018
Available online 19 May 2018

KEYWORDS

Fluorinated aminophosphonates;
Phenylalanine;
Phosphonate analogues;
DFT calculations;
X-ray analysis;
Hirshfeld surface analysis;
Cluster analysis

Abstract Due to their biological activity and structural analogy to corresponding α-amino acids, α-aminophosphonates and their fluorinated derivatives provide an important source for drug discovery. Therefore convenient access to this class of compounds is still desirable. Four series of novel phosphonate analogues of fluorinated phenylalanine containing variable number of fluorine atoms in different positions of the phenyl ring were synthesized and subjected to solid state characterization by single-crystal X-ray diffraction analysis, and to studies with the use of NMR, HRMS and DFT methods. Such an approach provided valuable information in regard to preferable conformation, hydrogen bonds and also weak intermolecular interactions present in the crystals investigated. As analogues of naturally occurring compounds, the obtained α-aminophosphonates have a big potential for biological activity. Formation of some indolinylphosphonates as minor products arisen from intramolecular S_NAr reactions show that aminophosphonates exhibiting an electronically depleted aromatic group, and possessing a fluorine atom in *ortho* position of the phosphonoalkyl substituent may give an entrance to further derivatives that may exhibit entirely new properties.

1. Introduction

α-Aminophosphonates are phosphorus analogues of naturally occurring amino acids. This class of compounds deserves special attention due to their biological and pharmacological properties. α-Aminophosphonates are known to act as enzyme inhibitors (Kafarski and Lejczak, 1991; Lejczak et al., 1989; Lombaert et al., 1995; Makhaeva et al., 2010), and exhibit antibacterial (Atherton et al., 1986; Kafarski and Lejczak, 1991), antifungal (Yang et al., 2006), antiviral (Song et al.,

* Corresponding authors.
E-mail addresses: jean-noel.volle@enscm.fr (J.-N. Volle), donatap@amu.edu.pl (D. Pluskota-Karwatka).
Peer review under responsibility of King Saud University.

Production and hosting by Elsevier

https://doi.org/10.1016/j.arabjc.2018.05.002

2003), and anticancer (Huang et al., 2013; Li et al., 2015; Wang et al., 2016) activities. The tetrahedral geometry of substituents around the phosphorus atom in α-aminophosphonates can be perceived as stable bioisostere of the transition state involved in the hydrolysis or enzymatic cleavage of ester (Bartlett et al., 1978; Bernhard and Orgel, 1959) or amide bonds (Kukhar and Hudson, 2000; Mucha et al., 2011). For these reasons, α-aminophosphonates are considered as valuable surrogates for enzyme inhibitors, and are very attractive compounds for studies focused on synthesis of bioactive derivatives.

Introduction of fluorine atoms into molecules of organic compound can result in richness of significant changes in biological properties and in metabolic stability of the modified molecules comparing to the non-fluorinated ones (Gillis et al., 2015; Smart, 2001). Moreover, ^{19}F NMR spectroscopy can be an useful tool in studying the interactions and metabolic transformations of fluorinated compounds in biological systems (Cobb and Murphy, 2009).

Therefore preparation of fluorine containing α-aminophosphonates of type **1** (Fig. 1), which are structural analogues of phenylalanine, and to our best knowledge are new compounds is desirable.

Recently it was reported that related α-aminophosphonates N-derivative (**2**, Fig. 1) can exhibit anticancer effect on tested cell lines (Wang et al., 2016), and that structurally similar compounds can potently inhibit protein tyrosine phosphatases with some selectivity (Wang et al., 2012). Fluorinated α-aminophosphonates of type **1** appear to be extremely interesting for biological studies. Presence of fluorine atoms in the phenyl ring may result in displaying of entirely new activities. For future evaluation of the compounds biological importance detailed knowledge of their structure is essential. Therefore in this work crystal structures of four series of fluorinated phosphonate analogues of phenylalanine were investigated by single-crystal X-ray diffraction analysis and using the quantum chemical calculations to estimate the energy of three conformers present in the crystals. Such an approach provided valuable information in regard to preferable conformation, hydrogen bonds as well as other interactions present in the crystals investigated.

Structural variations on α-aminophosphonates represented by general structure of compound **1** (Fig. 1) were achieved by formation of P-C-N bonds based on well known Kabachnik-Fields reaction (Cherkasov and Galkin, 1998; Khatri et al., 2017; Reddy et al., 2011; Rezaei et al., 2009) starting from a series of fluorinated aldehydes that differ in the number and position of fluorine atoms in the aromatic ring i.e. 2-(4-fluorophenyl)ethanal (**3a**), 2-(3,4,5-trifluorophenyl)ethanal (**3b**), 2-(2,4,6-trifluorophenyl)ethanal (**3c**) and 2-(2,3,4,5,6-pentafluorophenyl)ethanal (**3d**) which were subjected to reactions with various aniline derivatives and diethyl phosphite. It should be stressed that initial attempts to perform the typical three-component reactions, as well as syntheses under microwave irradiation and solvent-free conditions, and with application of several catalysts failed in the case of fluorinated aldehydes. Therefore our synthetic protocol was built on a two step reaction with imine as intermediate.

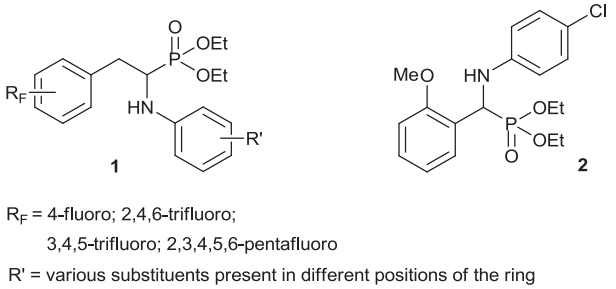

Fig. 1 Target α-aminophosphonates of type **1** and compound **2** exhibiting anticancer activity.

2. Experimental section

2.1. General methods

Reagent grade chemicals were used. Solvents were dried over 4 Å molecular sieves. All moisture sensitive reactions were carried out under nitrogen atmosphere with dry, freshly distilled reagents when possible. All glassware was carefully dried under vacuum with a flameless heat gun. TLC was performed on Merck Kieselgel 60-F254 with EtOAc/cyclohexane as eluent, and products were detected by UV light (254 nm) and with a solution of potassium permanganate. Merck Kieselgel 60 (230–400 mesh) was used for column chromatography. NMR spectra were recorded with instrument operating at 400 or 600 MHz (^{1}H), 101 MHz (^{13}C), 377 or 565 (^{19}F) and 162 or 243 MHz (^{31}P). Chemical shifts (δ) are given in ppm and calibrated from residual signals of $CDCl_3$ (7.26 ppm), acetone d_6 (2.09 ppm) for ^{1}H NMR and $CDCl_3$ (77.16 ppm) and acetone d_6 (29.84 ppm) for ^{13}C NMR. High resolution mass spectra were measured using electrospray ionization (ESI, positive-ion mode).

2.2. General procedure for the reduction of fluorinated phenylacetic acids

Under N_2 atmosphere, $LiAlH_4$ in dry diethyl ether (50 mL) was added to a 100 mL three-necked flask fitted with a reflux condenser. At 0 °C fluorinated phenylacetic acid diluted with dry diethyl ether (10 mL) was added dropwise, within 15 min to the flask. The reaction mixture was heated under reflux for 1 h and then cooled to 0 °C. Ice (10 mL) and H_2SO_4 (2 M, 10 mL) were added, and the mixture was filtered through a Celite pad, washed with diethyl ether, and the solvent was removed under reduced pressure.

*Synthesis of **4a**:* $LiAlH_4$ (2.56 g, 67.5 mmol), 4-fluorophenylacetic acid (7.0 g, 45 mmol).
*Synthesis of **4b**:* $LiAlH_4$ (0.33 g, 8.7 mmol), 2-(2,4,6-trifluorophenyl)acetic acid (1.1 g, 5.8 mmol).
*Synthesis of **4c**:* $LiAlH_4$ (1.48 g, 39 mmol), 2-(3,4,5-trifluorophenyl)acetic acid (5.0 g, 26 mmol).
*Synthesis of **4d**:* $LiAlH_4$ (1.25 g, 33 mmol), 2,3,4,5-penta fluorophenylacetic acid (5.0 g, 22 mmol).

2.2.1. 2-(4-fluorophenyl)ethanol (**4a**)

Yellow oil (6.3 g, 99%): ^{1}H NMR (400 MHz, $CDCl_3$) δ = 7.21–7.16 (m, 2H, 2 CHar), 7.03–6.92 (m, 2H, 2 CHar), 3.84 (t, 2H, J = 6.5 Hz, CH_2O), 2.84 (t, 2H, J = 6.5 Hz, CH_2), 1.43 (s, 1H, OH). ^{13}C NMR (101 MHz, $CDCl_3$) δ = 161.61

(d, J = 243.9 Hz, Car), 134.33 (s, Car), 130.39 (d, J = 7.9 Hz, 2 CHar), 115.23 (d, J = 21.1 Hz, 2 CHar), 63.43 (s, CH_2O), 38.24 (s, CH_2). ^{19}F NMR (377 MHz, $CDCl_3$) δ = −116.78 to −116.85 (m).

*2.2.2. 2-(2,4,6-trifluorophenyl)ethanol (**4b**)*

Yellow oil (1.0 g, 98%): ^1H NMR (400 MHz, $CDCl_3$) δ = 6.69–6.61 (m, 2H, 2 CHar), 3.82 (t, 2H, J = 6.7 Hz, CH_2O), 2.91 (t, 2H, J = 6.7 Hz, CH_2), 1.53 (s, 1H, OH). ^{13}C NMR (101 MHz, $CDCl_3$) δ = 163.29–162.54 (m, 2 Car), 160.83–160.08 (m, Car), 110.41 (d, J = 4.6 Hz, Car), 100.42–99.85 (m, 2 CHar), 61.83 (s, CH_2O), 25.79 (s, CH_2). ^{19}F NMR (377 MHz, $CDCl_3$) δ = −110.62 to −110.69 (m, 1F), −112.44 to −112.48 (m, 2F).

*2.2.3. 2-(3,4,5-trifluorophenyl)ethanol (**4c**)*

Yellow oil (4.5 g, 98%): ^1H NMR (400 MHz, $CDCl_3$) δ = 6.89–6.82 (m, 2H, 2 CHar), 3.85 (t, 2H, J = 6.4 Hz, OCH_2), 2.80 (t, 2H, J = 6.4 Hz, CH_2), 1.56 (s, 1H, OH). ^{13}C NMR (101 MHz, $CDCl_3$) δ = 152.48 (dd, J = 9.8, 4.1 Hz, 2 Car), 150.00 (dd, J = 10.0 Hz, 4.2 Hz, Car), 140.01–139.70 (m, Car), 113.01 (dd, J = 15.4, 5.6 Hz, 2 CHar), 63.00 (s, CH_2O), 38.43 (s, CH_2). ^{19}F NMR (377 MHz, $CDCl_3$) δ = −134.7 to −134.89 (m, 2F), −163.76 to −163.90 (m, 1F).

*2.2.4. 2-(perfluorophenyl)ethanol (**4d**)*

Colorless oil (4.5 g, 96%): ^1H NMR (400 MHz, $CDCl_3$) δ = 3.90–3.86 (m, 2H, CH_2O), 3.06–2.94 (m, 2H, CH_2), 1.48–1.46 (m, 1H, OH). ^{13}C NMR (101 MHz, $CDCl_3$) δ = 146.75–146.48 (m), 144.31–144.02 (m), 141.32–140.95 (m), 138.87–138.44 (m), 136.38–136.01 (m), 112.01–111.55 (m, Car), 61.05 (s, OCH_2), 25.79 (s, $ArCH_2$). ^{19}F NMR (377 MHz, $CDCl_3$) δ = −143.50 (dd, J = 22.5, 8.4 Hz, 2F), −156.91 (t, J = 20.8 Hz, 1F), −162.61 to −162.75 (m, 2F).

*2.3. General procedure for the oxidation of alcohols **4a-4d***

Under N_2 atmosphere and at 0 °C, Dess-Martin periodinane was added to a solution of alcohol in dry CH_2Cl_2 (7 mL), and the reaction mixture was stirred at room temperature for 2 h. Then, the reaction mixture was poured into 10 mL of distilled water and the phases were separated. The aqueous phase was neutralized by a saturated solution of $NaHCO_3$ and then extracted with CH_2Cl_2 (3 × 10 mL). The combined organic layers were dried over $MgSO_4$ and the solvent was removed under reduced pressure. The product was purified by column chromatography (silica gel, cyclohexane/ethyl acetate 1:1, v/v).

*Synthesis of **3a**:* Dess-Martin periodinane (2.7 g, 6.4 mmol), 2-(4-fluorophenyl)ethanol (0.6 g, 4.3 mmol).
*Synthesis of **3b**:* Dess-Martin periodinane (1.6 g, 3.8 mmol), 2-(2,4,6-trifluorophenyl)ethanol (0.5 g, 2.9 mmol).
*Synthesis of **3c**:* Dess-Martin periodinane (2.2 g, 5.3 mmol), 2-(3,4,5-trifluorophenyl)ethanol (0.7 g, 4.0 mmol).
*Synthesis of **3d**:* Dess-Martin periodinane (2.4 g, 5.6 mmol), 2-(perfluorophenyl)ethanol (0.8 g, 3.7 mmol).

*2.3.1. 2-(4-fluorophenyl)ethanal (**3a**)*

Pale yellow oil (0.34 g, 59%): ^1H NMR (400 MHz, $CDCl_3$) δ = 9.75 (t, 1H, J = 2.2 Hz, CHO), 7.21–7.16 (m, 2H, 2 CHar), 7.09–7.03 (m, 2H, 2 CHar), 3.68 (d, 2H, J = 2.1 Hz, CH_2). ^{19}F NMR (377 MHz, $CDCl_3$) δ = −115.08 to −115.17 (m).

*2.3.2. 2-(2,4,6-trifluorophenyl)ethanal (**3b**)*

Pale yellow oil (0.3 g, 61%): ^1H NMR (400 MHz, $CDCl_3$) δ = 9.74–9.74 (m, 1H, CHO), 6.75–6.68 (m, 2H, 2 CHar), 3.76 (s, 2H, CH_2). ^{19}F NMR (377 MHz, $CDCl_3$) δ = −108.30 to −108.38 (m, 1F), −111.29 (t, J = 6.7 Hz, 2F).

*2.3.3. 2-(3,4,5-trifluorophenyl)ethanal (**3c**)*

Yellow oil (0.4 g, 69%): ^1H NMR (400 MHz, $CDCl_3$) δ = 9.76 (t, 1H, J = 1.7 Hz, CHO), 6.89–6.81 (m, 1H, 2 CHar), 3.68 (s, 1H, CH_2). ^{19}F NMR (377 MHz, $CDCl_3$) δ = −133.58 to −133.69 (m, 2F), −161.83 (tm, 1F, J = 20.5 Hz).

*2.3.4. 2-(perfluorophenyl)ethanal (**3d**)*

Yellow oil (0.42 g, 52%): ^1H NMR (400 MHz, $CDCl_3$) δ = 9.77 (s broad, 1H, CHO), 3.88–3.87 (m, 2H, CH_2). ^{19}F NMR (377 MHz, $CDCl_3$) δ = −141.89 to −141.98 (m, 2F), −154.45 (t, 1F, J = 20.8 Hz), −161.76 to −161.91 (m, 2F).

2.4. General procedure for the preparation of aminophosphonates

To the mixture of aldehyde **3a-3d** in dry toluene (10 mL), aniline or derivatives were added dropwise under a N_2 atmosphere. The reaction mixture was heated under reflux for 4 h, then, $HP(O)(OEt)_2$ and NaH were added, and the mixture refluxed for 3–18 h. After cooling to room temperature, the solvent was removed under reduced pressure, and the crude was purified by column chromatography (cyclohexane/ethyl acetate 1:1, v/v).

Synthesis of 4-fluorophenyl derivatives of α-aminophosphonates.

2-(4-fluorophenyl)ethanal (0.1 g, 0.7 mmol), aniline or derivatives (0.7 mmol), $HP(O)(OEt)_2$ (0.18 mL, 1.4 mmol), NaH (0.034 g, 1.4 mmol).

Synthesis of 2,4,6-trifluorophenyl and 3,4,5-trifluorophenyl derivatives of α-aminophosphonates.

Aldehyde (0.1 g, 0.57 mmol), aniline or derivatives (0.57 mmol), $HP(O)(OEt)_2$ (0.15 mL, 1.14 mmol), NaH (0.027 g, 1.14 mmol).

Synthesis of perfluorophenyl derivatives of α-aminophosphonates.

2-(perfluorophenyl)ethanal (0.1 g, 0.48 mmol), aniline or derivatives (0.48 mmol), $HP(O)(OEt)_2$ (0.12 mL, 0.96 mmol), NaH (0.023 g, 0.96 mmol).

*2.4.1. Diethyl (2-(4-fluorophenyl)-1-(phenylamino)ethyl) phosphonate (**1a**)*

Pale yellow solid (51 mg, 21%): ^1H NMR (400 MHz, $CDCl_3$) δ = 7.20–7.17 (m, 2H, J = 8.5 Hz, 5.5 Hz, 2 CHar), 7.10 (t, 2H, J = 7.8 Hz, 2 CHar), 6.91 (t, 2H, J = 8.6 Hz, 2 CHar), 6.68 (t, 1H, J = 7.3 Hz, CHar), 6.53 (d, 2H, J = 8.0 Hz, 2 CHar), 4.13–3.90 (m, 5H, 2 OCH_2, CH), 3.82 (s broad, 1H, NH), 3.22 (td, 1H, J = 13.7 Hz, 4.7 Hz, $ArCH_2$), 2.99–2.91 (m, 1H, $ArCH_2$), 1.25 (t, 3H, J = 7.1 Hz, CH_3), 1.15 (t, 3H, J = 7.1 Hz, CH_3). ^{13}C NMR (101 MHz, $CDCl_3$) δ = 161.85 (d, J = 244.6 Hz, Car), 146.77 (d, J = 6.0 Hz, Car), 133.16 (d, J = 8.6 Hz, Car), 130.97 (d, J = 7.9 Hz, 2 CHar), 129.30

(s, 2 CHar), 118.42 (s, CHar), 115.19 (d, J = 21.2 Hz, 2 CHar), 113.67 (s, 2 CHar), 63.03 (d, J = 7.1 Hz, OCH_2), 62.18 (d, J = 7.3 Hz, OCH_2), 52.59 (d, J = 155.6 Hz, CHP), 35.69 (d, J = 4.5 Hz, $ArCH_2$), 16.50, 16.46, 16.44 and 16.40 (2 CH_3). ^{19}F NMR (377 MHz, $CDCl_3$) δ = −116.42 to −116.49 (m). ^{31}P NMR (162 MHz, $CDCl_3$) δ = 24.82 (s). HRMS (ESI^+) calcd. for $C_{18}H_{24}FNO_3P([M+H]^+)$: 352.1478, found: 352.1475.

2.4.2. Diethyl (1-((4-chlorophenyl)amino)-2-(4-fluorophenyl) ethyl)phosphonate (*1b*)

Pale yellow solid (53 mg, 20%): ^{1}H NMR (400 MHz, $CDCl_3$) δ = 7.18–7.14 (m, 2H, 2 CHar), 7.03–7.01 (m, 2H, 2 CHar), 6.93–6.90 (m, 2H, 2 CHar), 6.43 (d, 2H, J = 8.8 Hz, 2 CHar), 4.13–3.81 (m, 6H, 2 OCH_2, CH, NH), 3.21–3.17 (m, 1H, $ArCH_2$), 2.96–2.87 (m, 1H, $ArCH_2$), 1.26 (t, 3H, J = 7.1 Hz, CH_3), 1.16 (t, 3H, J = 7.0 Hz, 3.3 Hz, CH_3). ^{13}C NMR (101 MHz, $CDCl_3$) δ = 161.88 (d, J = 244.9 Hz, Car), 145.55–145.47 (m, Car), 132.99 (d, J = 12.8 Hz, Car), 130.87 (d, J = 7.9 Hz, 2 CHar), 129.10 (s, 2 CHar), 122.80 (s, Car), 115.29 (d, J = 21.3 Hz, 2 CHar), 114.64 (s, 2 CHar), 63.10 (d, J = 7.1 Hz, OCH_2), 62.28 (d, J = 7.4 Hz, OCH_2), 52.87 (d, J = 156.3 Hz, CH), 35.67 (d, J = 4.5 Hz, $ArCH_2$), 16.55, 16.50 and 16.45 (2 CH_3). ^{19}F NMR (377 MHz, $CDCl_3$) δ = −116.13 to −116.20 (m). ^{31}P NMR (162 MHz, $CDCl_3$) δ = 24.49–24.44 (m). HRMS (ESI^+) calcd. for $C_{18}H_{23}ClFNO_3P$ ($[M+H]^+$): 386.1088, found: 386.1087.

2.4.3. (2-(4-Fluorophenyl)-1-(o-tolylamino)ethyl)phosphonate (*1c*)

White solid (52 mg, 20%): ^{1}H NMR (400 MHz, $CDCl_3$) δ = 7.20–7.16 (m, 2H, 2 CHar), 7.01–6.94 (m, 2H, 2 CHar), 6.92 (t, 2H, J = 8.6 Hz, 2 CHar), 6.64 (t, 1H, J = 7.3 Hz, CHar), 6.55 (d, 1H, J = 8.1 Hz, CHar), 4.13–3.88 (m, 5H, 2 OCH_2, CH), 3.66–3.64 (m, 1H, NH), 3.27–3.23 (td, 1H, J = 14.0, 14.9 Hz, $ArCH_2$), 3.04–2.96 (m, 1H, $ArCH_2$), 2.06 (s, 3H, $ArCH_3$), 1.24 (t, 3H, J = 7.1 Hz, CH_3), 1.16 (t, 3H, J = 7.1 Hz, CH_3). ^{13}C NMR (101 MHz, $CDCl_3$) δ = 161.90 (d, J = 244.7 Hz, Car), 144.72 (d, J = 5.8 Hz, Car), 133.08 (dd, J = 11.2, 3.2 Hz, Car), 130.99 (d, J = 7.9 Hz, 2 CHar), 130.44 (s, CHar), 127.12 (s, CHar), 122.55 (s, Car), 118.00 (s, CHar), 115.20 (d, J = 21.2 Hz, 2 CHar), 110.95 (s, CHar), 62.93 (d, J = 7.1 Hz, OCH_2), 62.26 (d, J = 7.2 Hz, OCH_2), 52.48 (d, J = 155.8 Hz, CHP), 35.60 (d, J = 4.1 Hz, $ArCH_2$), 17.46 (s, $ArCH_3$), 16.49, 16.43 (2 CH_3). ^{19}F NMR (377 MHz, $CDCl_3$) δ = −116.38 to −116.41 (m). ^{31}P NMR (162 MHz, $CDCl_3$) δ = 24.89 (s). HRMS (ESI^+) calcd. for $C_{19}H_{26}FNO_3P$ ($[M+H]^+$): 366.1634, found: 366.1633.

2.4.4. (2-(4-Fluorophenyl)-1-(m-tolylamino)ethyl)phosphonate (*1d*)

Yellow solid (64 mg, 25%): ^{1}H NMR (400 MHz, $CDCl_3$) δ = 7.19–7.17 (m, 2H, 2 CHar), 7.00–6.98 (m, 1H, CHar), 6.95–6.90 (m, 2H, 2 CHar), 6.52 (d, 1H, J = 7.4 Hz, CHar), 6.35–6.34 (m, 2H, 2 CHar), 4.12–3.75 (m, 5H, 2 OCH_2, CH), 3.75 (s, 1H, NH), 3.25–3.18 (td, 1H, J = 13.9, 4.8 Hz, $ArCH_2$), 2.99–2.89 (m, 1H, $ArCH_2$), 2.22 (s, 3H, $ArCH_3$), 1.25 (t, 3H, J = 7.1 Hz, CH_3), 1.16 (t, 3H, J = 7.1 Hz, CH_3). ^{13}C NMR (101 MHz, $CDCl_3$) δ = 161.91 (d, J = 244.6 Hz, Car), 146.74 (d, J = 6.4 Hz, Car), 139.12 (s, Car), 133.23 (d, J = 14.6 Hz, Car), 131.06 (d, J = 7.9 Hz, 2 CHar), 129.19 (s, CHar), 119.42 (s, CHar), 115.21 (d, J = 21.2 Hz, 2 CHar), 114.55 (s, CHar), 110.82 (s, CHar), 63.07 (d, J = 7.1 Hz, OCH_2), 62.23 (d, J = 7.3 Hz, OCH_2), 52.55 (d, J = 155.6 Hz, CHP), 35.77 (d, J = 4.4 Hz, $ArCH_2$), 21.66 (s, $ArCH_3$), 16.55, 16.51, 16.49 and 16.45 (2 CH_3). ^{19}F NMR (377 MHz, $CDCl_3$) δ = −116.52 to −116.59 (m). ^{31}P NMR (162 MHz, $CDCl_3$) δ = 24.86 (s). HRMS (ESI^+) calcd. for $C_{19}H_{26}FNO_3P$ ($[M+H]^+$): 366.1634, found: 366.1635.

2.4.5. (2-(4-Fluorophenyl)-1-(p-tolylamino)ethyl)phosphonate (*1e*)

Pale yellow solid (71 mg, 28%): ^{1}H NMR (400 MHz, $CDCl_3$) δ = 7.19–7.17 (m, 2H, 2 CHar), 6.94–6.90 (m, 4H, 4 CHar), 6.46 (d, 1H, J = 8.4 Hz, 2 CHar), 4.13–3.87 (m, 5H, 2 OCH_2, CH), 3.69 (s, 1H, NH), 3.21 (td, J = 13.9 Hz, 4.8 Hz, 1H, $ArCH_2$), 2.98–2.90 (m, 1H, $ArCH_2$), 2.20 (s, 3H, $ArCH_3$), 1.25 (t, 3H, J = 7.1 Hz, CH_3), 1.16 (t, 3H, J = 7.1 Hz, CH_3). ^{13}C NMR (101 MHz, $CDCl_3$) δ = 161.55 (d, J = 244.5 Hz, Car), 144.43 (d, J = 6.5 Hz, Car), 133.23 (dd, J = 11.3, 3.2 Hz, Car), 131.01 (d, J = 7.9 Hz, 2 CHar), 129.81 (s, 2 CHar), 127.67 (s, Car), 115.16 (d, J = 21.2 Hz, 2 CHar), 113.85 (s, 2 CHar), 63.00 (d, J = 7.0 Hz, OCH_2), 62.16 (d, J = 7.3 Hz, OCH_2), 52.97 (d, J = 155.6 Hz, CHP), 35.65 (d, J = 4.5 Hz, $ArCH_2$), 20.44 (s, $ArCH_3$), 16.53, 16.47 and 16.41 (2 CH_3). ^{19}F NMR (377 MHz, $CDCl_3$) δ = −116.50 to −116.57 (m). ^{31}P NMR (162 MHz, $CDCl_3$) δ 24.99 (s). HRMS (ESI^+) calcd. for $C_{19}H_{26}FNO_3P$ ($[M+H]^+$): 366.1634, found: 366.1635.

2.4.6. (2-(4-Fluorophenyl)-1-(p-nitrophenyl)ethyl)phosphonate (*1f*)

Yellow solid (75 mg, 27%): ^{1}H NMR (400 MHz, $CDCl_3$) δ = 7.97–7.95 (m, 2H, 2 CHar), 7.19–7.16 (m, 2H, 2 CHar), 6.91–6.87 (m, 2H, 2 CHar), 6.50 (d, 2H, J = 8.3 Hz, 2 CHar), 5.70–5.54 (m, 1H, NH) 4.18–3.95 (m, 5H, 2 OCH_2,CH), 3.28–3.21 (m, 1H, $ArCH_2$), 3.02–2.94 (m, 1H, $ArCH_2$), 1.34 (t, 3H, J = 7.1 Hz, CH_3), 1.15 (t, 3H, J = 7.1 Hz, CH_3). ^{13}C NMR (101 MHz, $CDCl_3$) δ = 161.96 (d, J = 245.6 Hz, Car), 152.74 (s, Car), 138.45 (s, Car), 132.55 (d, J = 13.9 Hz, Car), 130.73 (d, J = 8.0 Hz, 2 CHar), 126.24 (s, 2 CHar), 115.49 (d, J = 21.3 Hz, 2 CHar), 111.62 (s, 2 CHar), 63.49 (d, J = 7.2 Hz, OCH_2), 62.66 (d, J = 7.6 Hz, OCH_2), 52.15 (d, J = 158.1 Hz, CHP), 35.53 (s, $ArCH_2$), 16.59, 16.58, 16.54, 16.53 (2 CH_3). ^{19}F NMR (377 MHz, $CDCl_3$) δ = −115.31 to −115.39 (m). ^{31}P NMR (162 MHz, $CDCl_3$) δ = 23.22 (s). HRMS (ESI^+) calcd. for $C_{18}H_{23}FN_2O_5P$ ($[M+H]^+$): 397.1329, found: 397.1327.

2.4.7. Diethyl (2-(2,4,6-trifluorophenyl)-1-(phenylamino) ethyl)phosphonate (*1g*)

Yellow solid (48 mg, 22%): ^{1}H NMR (400 MHz, $CDCl_3$) δ = 7.05 (t, 2H, J = 7.8 Hz, 2 CHar), 6.64 (t, 1H, J = 7.3 Hz, CHar), 6.56–6.49 (m, 4H, 4 CHar), 4.19–3.97 (m, 5H, CH, 2 OCH_2), 3.80–3.77 (m, 1H, NH), 3.20–3.14 (m, 1H, $ArCH_2$), 3.09–3.00 (m, 1H, $ArCH_2$), 1.29 (t, 3H, J = 7.1 Hz, CH_3), 1.20 (t, 3H, J = 7.0 Hz, CH_3) ppm. ^{13}C NMR (101 MHz, $CDCl_3$) δ = 163.10–162.90 (m, 2 Car), 160.75–160.49 (m, Car), 146.74 (d, J = 5.9 Hz, Car), 129.24 (s, 2 CHar), 118.44 (s, CHar), 113.38 (s, 2 CHar), 110.31–110.16 (m, Car), 100.34–99.78 (m, 2 CHar), 63.45 (d, J = 6.9 Hz, OCH_2), 62.34 (d, J = 7.4 Hz, OCH_2), 50.93 (d, J = 157.1 Hz, CH), 23.97 (d, J = 6.9 Hz, $ArCH_2$), 16.61, 16.55, 16.53, and 16.47

(2 CH_3) ppm. ^{19}F NMR (377 MHz, $CDCl_3$) δ = −109.89 (t, 1F, J = 5.8 Hz), −112.09 (d, 2F, J = 5.8 Hz) ppm. ^{31}P NMR (162 MHz, $CDCl_3$) δ = 24.19 (s) ppm. HRMS (ESI^+) calcd. for $C_{18}H_{22}F_3NO_3P$ ($[M+H]^+$): 388.1289, found: 388.1288.

2.4.8. (2-(2,4,6-Trifluorophenyl) 1-((4-chlorophenyl)amino) ethyl)phosphonate (**1h**)

White solid (0.66 mg, 27%): ^1H NMR (400 MHz, $CDCl_3$) δ = 6.99 (d, 2H, J = 8.8 Hz, 2 CHar), 6.59–6.42 (m, 2H, 2 CHar), 6.43 (d, 2H, J = 8.8 Hz, 2 CHar), 4.16–3.82 (m, 6H, CH, 2 OCH_2, NH), 3.19–3.13 (m, 1H, $ArCH_2$), 3.06–2.97 (m, 1H, $ArCH_2$), 1.30 (t, 3H, J = 7.1 Hz, CH_3), 1.20 (t, 3H, J = 7.1 Hz, CH_3). ^{13}C NMR (101 MHz, $CDCl_3$) δ = 163.13–162.81 (m, 2 Car), 160.67–160.33 (m, Car), 145.37 (d, J = 5.8 Hz, Car), 129.07 (s, 2 CHar), 122.90 (s, Car), 114.33 (s, 2 CHar), 109.84–109.65 (m, Car), 100.40–99.84 (m, 2 CHar), 63.45 (d, J = 7.0 Hz, OCH_2), 62.43 (d, J = 7.5 Hz, OCH_2), 51.14 (d, J = 157.8 Hz, CHP), 23.86 (d, J = 6.7 Hz, $ArCH_2$), 16.62, 16.57, 16.53 and 16.47 (2 CH_3). ^{19}F NMR (377 MHz, $CDCl_3$) δ = −109.37 to −109.40 (m, 1F), −112.16 (d, 2F, J = 5.9 Hz). ^{31}P NMR (162 MHz, $CDCl_3$) δ = 23.80–23.69 (m). HRMS (ESI^+) calcd. for $C_{18}H_{21}ClF_3NO_3P$ ($[M+H]^+$): 422.0900, found: 422.0898.

2.4.9. (2-(2,4,6-Trifluorophenyl)-1-(o-tolylamino)ethyl) phosphonate (**1i**)

Yellow oil (81 mg, 35%): ^1H NMR (400 MHz, $CDCl_3$) δ = 6.98–6.95 (m, 2H, 2 CHar), 6.59–6.50 (m, 4H, 4 CHar), 4.18–3.92 (m, 5H, 2 OCH_2, CH), 3.72 (dd, 1H, J = 10.3, 3.6 Hz, NH), 3.26–3.18 (m, 1H, $ArCH_2$), 3.14–3.05 (m, 1H, $ArCH_2$), 2.11 (s, 3H, $ArCH_3$), 1.28 (t, 3H, J = 7.1 Hz, CH_3), 1.18 (t, 3H, J = 7.1 Hz, CH_3). ^{13}C NMR (101 MHz, $CDCl_3$) δ = 160.82 (ddd, J = 247.2 Hz, 14.8 Hz, 11.4 Hz, 2 Car), 160.55 (dt, J = 248.6 Hz, 15.7 Hz, Car),143.43 (d, J = 4.4 Hz, Car), 129.22 (s, CHar), 125.81 (s, CHar), 121.19 (s, Car), 116.65 (s, CHar), 109.26 (s, CHar), 108.92–108.74 (m, Car), 99.18–98.62 (m, 2 CHar), 62.09 (d, J = 7.1 Hz, OCH_2), 61.19 (d, J = 7.4 Hz, OCH_2), 49.32 (d, J = 156.0 Hz, CHP), 22.89 (d, J = 6.6 Hz, $ArCH_2$), 16.23 (s, $ArCH_3$), 15.38, 15.34, 15.33 and 15.29 (2 CH_3). ^{19}F NMR (377 MHz, $CDCl_3$) δ = −109.83 (t, 1F, J = 5.8 Hz), −111.88 (d, 2F, J = 5.8 Hz). ^{31}P NMR (162 MHz, $CDCl_3$) δ = 24.29 (s). HRMS (ESI^+) calcd. for $C_{19}H_{24}F_3NO_3P$ ($[M+H]^+$): 402.1446, found: 402.1450.

2.4.10. (2-(2,4,6-Trifluorophenyl)-1-(m-tolylamino)ethyl) phosphonate (**1j**)

Yellow solid (35 mg, 15%): ^1H NMR (400 MHz, $CDCl_3$) δ = 6.96–6.92 (m, 1H, CHar), 6.58–6.51 (m, 2H, 2 CHar), 6.46 (d, 1H, J = 7.5 Hz, CHar), 6.34–6.32 (m, 2H, 2 CHar), 4.17–3.99 (m, 5H, 2 OCH_2, CH), 3.74 (d, 1H, J = 8.0 Hz, NH), 3.19–3.13 (m, 1H, $ArCH_2$), 3.08–2.99 (m, 1H, $ArCH_2$), 2.19 (s, 3H, $ArCH_3$), 1.29 (t, 3H, J = 7.1 Hz, CH_3), 1.20 (t, 3H, J = 7.1 Hz, CH_3). ^{13}C NMR (101 MHz, $CDCl_3$) δ = 161.9 (ddd, J = 247.4 Hz, 11.5 Hz, 2 Car), 161.73 (dt, J = 248.2 Hz, 15.8 Hz, Car), 146.70 (d, J = 6.1 Hz, Car), 138.97 (s, Car), 129.07 (s, CHar), 119.33 (s, CHar), 114.17 (s, CHar), 110.54 (s, CHar), 110.15–109.91 (m, Car), 100.28–99.72 (m, 2 CHar), 63.43 (d, J = 7.0 Hz, OCH_2), 62.30 (d, J = 7.4 Hz, OCH_2), 50.85 (d, J = 156.8 Hz, CHP), 23.98 (d, J = 6.9 Hz, $ArCH_2$), 21.59 (s, $ArCH_3$), 16.60, 16.54, 16.51 and 16.46 (2 CH_3). ^{19}F NMR (377 MHz, $CDCl_3$) δ = −109.99 (t, 1F, J = 5.9 Hz), −112.02 to −112.03 (m, 2F). ^{31}P NMR (162 MHz, $CDCl_3$) δ = 24.27 (s). HRMS (ESI^+). for $C_{19}H_{24}F_3NO_3P$ ($[M+H]^+$): 402.1446, found: 402.1442.

2.4.11. Diethyl (2-(3,4,5-trifluorophenyl)-1-(phenylamino) ethyl)phosphonate (**1k**)

Pale yellow solid (48 mg, 22%): ^1H NMR (400 MHz, $CDCl_3$) δ = 7.13 (t, 2H, J = 7.9 Hz, 2 CHar), 6.90–6.83 (m, 2H, 2 CHar), 6.72 (t, 1H, J = 7.3 Hz, CHar), 6.55 (d, 2H, J = 8.1 Hz, 2 CHar), 4.14–3.86 (m, 6H, 2 OCH_2,CH, NH), 3.21–3.13 (td, 1H, J = 13.7, 4.3 Hz, $ArCH_2$), 2.94–2.86 (m, 1H, $ArCH_2$), 1.27 (t, 3H, J = 7.1 Hz, CH_3), 1.17 (t, 3H, J = 7.1 Hz, CH_3). ^{13}C NMR (101 MHz, $CDCl_3$) δ = 150.99 (ddd, J = 249.6 Hz, 9.9 Hz, 4.3 Hz, 2 Car), 147.05–145.17 (m, Car), 138.76 (dt, J = 250.1 Hz, 30.3 Hz, 15.4 Hz, Car), 135.08–132.42 (m, Car), 129.49 (s, 2 CHar), 118.86 (s, CHar), 113.74, 113.69, 113.59 and 113.53 (m, 4 CHar), 63.24 (d, J = 7.0 Hz, OCH_2), 62.38 (d, J = 7.3 Hz, OCH_2), 52.22 (d, J = 155.4 Hz, CHP), 35.97 (d, J = 4.5 Hz, $ArCH_2$), 16.52, 16.48, 16.47 and 16.42 (2 CH_3). ^{19}F NMR (377 MHz, $CDCl_3$) δ = −134.85 (d, 2F, J = 20.5 Hz), −163.25 (t, 1F, J = 20.6 Hz). ^{31}P NMR (162 MHz, $CDCl_3$) δ = 24.10 (s). HRMS (ESI^+) calcd. for $C_{18}H_{22}F_3NO_3P$ ($[M+H]^+$): 388.1289, found: 388.1286.

2.4.12. (2-(3,4,5-Trifluorophenyl) 1-((4-chlorophenyl)amino) ethyl)phosphonate (**1l**)

Pale yellow solid (53 mg, 22%): ^1H NMR (400 MHz, $CDCl_3$) δ = 7.09–7.06 (m, 2H, 2 CHar), 6.87–6.85 (m, 2H, 2 CHar), 6.48–6.46 (m, 2H, 2 CHar), 4.14–3.82 (m, 6H, 2 OCH_2,CH, NH), 3.17–3.12 (m, 1H, $ArCH_2$), 2.92–2.84 (m, 1H, $ArCH_2$), 1.28 (t, 3H, J = 7.1 Hz, CH_3), 1.18 (t, 3H, J = 7.1 Hz, CH_3). ^{13}C NMR (101 MHz, $CDCl_3$) δ = = 151.03 (ddd, J = 250.0 Hz, 10.2 Hz, 4.3 Hz, 2Car), 145.14 (s, Car), 138.86 (dt, 253.6 Hz, 10.3 Hz, 6.7 Hz, Car), 133.72–133.61 (m, Car), 129.35 (s, 2 CHar), 123.37 (s, Car), 114.72 (s, 2 CHar), 113.57 (dd, J = 15.6, 5.7 Hz, 2 CHar), 63.32 (d, J = 7.1 Hz, OCH_2), 62.50 (d, J = 7.4 Hz, OCH_2), 52.45 (d, J = 156.0 H z, CHP), 35.91 (d, J = 4.6 Hz, $ArCH_2$), 16.59, 16.54 and 16.48 (2 CH_3). ^{19}F NMR (377 MHz, $CDCl_3$) δ = −134.52 (d, 2F, J = 20.5 Hz), −162.86 (t, 1F, J = 20.6 Hz). ^{31}P NMR (162 MHz, $CDCl_3$) δ 23.74 (s). HRMS (ESI^+) calcd. for $C_{18}H_{21}ClF_3NO_3P$ ($[M+H]^+$: 422.0900, found: 422.0898.

2.4.13. Diethyl (2-(3,4,5-trifluorophenyl)-1-(o-tolylamino) ethyl)phosphonate (**1m**)

White solid (61 mg, 27%): ^1H NMR (400 MHz, $CDCl_3$) δ = 7.08–7.03 (m, 2H, 2 CHar), 6.89–6.81 (m, 2H, 2 CHar), 6.67 (t, 1H, J = 7.4 Hz, CHar), 6.53 (d, 1H, J = 8.0 Hz, CHar), 4.12–3.92 (m, 5H, 2 OCH_2, CH), 3.70–3.66 (m, 1H, NH), 3.24– 3.17 (td, 1H, J = 14.3, 4.9 Hz, $ArCH_2$), 2.98–2.90 (m, 1H, $ArCH_2$), 2.10 (s, 3H, $ArCH_3$), 1.25 (t, 3H, J = 7.1 Hz, CH_3), 1.17 (t, 3H, J = 7.1 Hz, CH_3). ^{13}C NMR (101 MHz, $CDCl_3$) δ = 150.95 (ddd, J = 249.6, 9.8, 4.0 Hz, 2 Car), 144.27 (d, J = 6.0 Hz, Car), 138.75 (dt, J = 250.3 Hz, 30.6 Hz, 15.3 Hz, Car), 134.02–133.67 (m, Car),130.68 (s, CHar), 127.22 (s, CHar), 122.68 (s, Car), 118.43 (s, CHar), 113.70–113.49 (m, 2 CHar), 110.90 (s, CHar), 63.05 (d, J = 7.1 Hz, OCH_2), 62.44 (d, J = 7.2 Hz, OCH_2), 52.01 (d, J = 154.9 H z, CHP), 35.83 (d, J = 4.1 Hz, $ArCH_2$), 17.45 (s, $ArCH_3$),

16.46, 16.45, 16.40 and 16.39 (2 CH_3). ^{19}F NMR (377 MHz, $CDCl_3$) δ = −134.91 (d, 2F, J = 20.5 Hz), −163.21 (t, 1F, J = 20.5 Hz). ^{31}P NMR (162 MHz, $CDCl_3$) δ = 24.18 (s). HRMS (ESI^+) calcd. for $C_{19}H_{24}F_3NO_3P$ $([M+H])^+$): 402.1446, found: 402.1443.

*2.4.14. (2-(3,4,5-Trifluorophenyl)-1-(m-tolylamino)ethyl) phosphonate (**1n**)*

Yellow oil (34 mg, 15%): ^1H NMR (400 MHz, $CDCl_3$) δ = 7.02 (dd, 1H, J = 7.9 Hz, CHar), 6.90–6.83 (m, 2H, 2 CHar), 6.55 (d, 1H, J = 7.5 Hz, CHar), 6.37–6.35 (m, 2H, 2 CHar), 4.14–3.75 (m, 5H, 2 OCH_2, CH), 3.75 (s, 1H, NH), 3.17 (td, 1H, J = 14.0, 4.8 Hz, $ArCH_2$), 2.93–2.85 (m, 1H, $ArCH_2$), 2.24 (s, 3H, $ArCH_3$), 1.27 (t, 3H, J = 7.1 Hz, CH_3), 1.18 (t, 3H, J = 7.1 Hz, CH_3). ^{13}C NMR (101 MHz, $CDCl_3$) δ = 149.15 (ddd, J = 249.5 Hz, 11.6 Hz, 4.0 Hz, 2 Car), 146.20 (d, J = 6.7 Hz, Car), 139.20 (s, Car), 138.65 (dt, J = 251.6 H z, 8.5 Hz, 4.9 Hz, Car), 133.97–133.71 (m, Car), 129.23 (s, CHar), 119.71 (s, CHar), 114.49 (s, CHar), 113.67–113.46 (m, 2 Car), 110.71 (s, CHar), 63.10 (d, J = 7.0 Hz, OCH_2), 62.26 (d, J = 7.3 Hz, OCH_2), 52.01 (d, J = 155.6 Hz, CHP), 35.92 (s, $ArCH_2$), 21.53 (s, $ArCH_3$), 16.41, 16.37, 16.36 and 16.31(2 CH_3). ^{19}F NMR (377 MHz, $CDCl_3$) δ = −134.97 (d, 2F, J = 20.5 Hz), −163.39 (t, 1F, J = 20.5 Hz). ^{31}P NMR (162 MHz, $CDCl_3$) δ = 24.13 (s). HRMS (ESI^+) calcd. for $C_{19}H_{24}F_3NO_3P$ $([M+H])^+$): 402.1446, found: 402.1444.

*2.4.15. (2-(3,4,5-Trifluorophenyl)-1-(p-tolylamino)ethyl) phosphonate (**1o**)*

Yellow solid (45 mg, 20%): ^1H NMR (400 MHz, $CDCl_3$) δ = 6.95 (d, 2H, J = 8.3 Hz, 2 CHar), 6.90–6.82 (m, 2H, 2 CHar), 6.47 (d, 2H, J = 8.4 Hz, 2 CHar), 4.12–3.86 (m, 5H, 2 OCH_2, CH), 3.72 (s, 1H, NH), 3.15 (td, 1H, J = 14.0, 4.8 Hz, $ArCH_2$), 2.93–2.85 (m, 1H, $ArCH_2$), 2.21 (s, 3H, $ArCH_3$), 1.26 (t, 3H, J = 7.1 Hz, CH_3), 1.18 (t, 3H, J = 7.1 Hz, CH_3). ^{13}C NMR (101 MHz, $CDCl_3$) δ = 150.66 (ddd, J = 249.4 Hz, 9.9 Hz, 4.0 Hz, 2 Car), 143.92 (d, J = 8.1 Hz, Car), 138.54 (dt, J = 250.1 Hz, 30.6 Hz, 15.2 Hz, Car), 137.53–137.23 (m, Car), 129.86 (s, 2 CHar), 128.03 (s, Car), 113.81 (s, 2 CHar), 113.65–113.44 (m, 2 CHar), 63.09 (d, J = 7.0 Hz, OCH_2), 62.23 (d, J = 7.3 Hz, OCH_2), 52.47 (d, J = 155.3 Hz, CHP), 35.81 (d, J = 4.5 Hz, $ArCH_2$), 20.35 (s, $ArCH_3$), 16.42 and 16.37 (2 CH_3). ^{19}F NMR (377 MHz, $CDCl_3$) δ = −134.95 (d, 2F, J = 20.5 Hz), −163.37 (t, 1F, J = 20.5 Hz). ^{31}P NMR (162 MHz, $CDCl_3$) δ = 24.27 (s). HRMS (ESI^+) calcd. for $C_{19}H_{24}F_3NO_3P$ $([M+H])^+$): 402.1446, found: 402.1442.

*2.4.16. (2-(3,4,5-Trifluorophenyl)-1-(p-nitrophenyl)ethyl) phosphonate (**1p**)*

Yellow oil (50 mg, 20%): ^1H NMR (400 MHz, $CDCl_3$) δ = 7.98 (d, 2H, J = 9.1 Hz, 2 CHar), 6.80–6.76 (m, 2H, 2 CHar), 6.45 (d, 2H, J = 9.1 Hz, 2 CHar), 4.60 (s, 1H, NH), 4.11–3.92 (m, 4H, 2 OCH_2, CH), 3.17–3.13 (m, 1H, $ArCH_2$), 2.89–2.81 (m, 1H, $ArCH_2$), 1.26 (t, 3H, J = 7.1 Hz, CH_3), 1.13 (t, 3H, J = 7.1 Hz, CH_3). ^{13}C NMR (101 MHz, $CDCl_3$) δ = 152.44–149.89 (m, 3 Car), 138.88 (dt, J = 251.0 Hz, 30.2 Hz, 15.0 Hz, Car), 138.79 (s, Car), 133.39–133.05 (m, Car), 126.37 (s, 2 CHar), 113.59–113.38 (m, 2 CHar) 111.65 (s, 2 CHar), 63.78 (d, J = 7.3 Hz, OCH_2), 62.89 (d, J = 7.7 Hz, OCH_2), 51.74 (d, J = 159.2 Hz, CHP), 35.56 (s, $ArCH_2$), 16.62 and 16.57 (2 CH_3). ^{19}F NMR (377 MHz, $CDCl_3$) δ = −134.10 to −134.19 (m, 2F), −162.23 to −162.37 (m, 1F). ^{31}P NMR (162 MHz, $CDCl_3$) δ = 22.41 (s). HRMS (ESI^+) calcd. for $C_{18}H_{21}F_3N_2O_5P$ $([M+H])^+$): 433.1140, found: 433.1140.

*2.4.17. Diethyl (2-(perfluorophenyl)-1-(phenylamino)ethyl) phosphonate (**1q**)*

White solid (100 mg, 49%): ^1H NMR (400 MHz, $CDCl_3$) δ = 7.11–7.07 (m, 2H, 2CHar), 6.68 (t, 1H, J = 7.4 Hz, CHar), 6.53 (d, 2H, J = 7.8 Hz, 2 CHar), 4.18–4.00 (m, 5H, 2 OCH_2, CH), 3.81–3.78 (m, 1H, NH), 3.25–3.10 (m, 2H, $ArCH_2$), 1.30 (t, 3H, J = 7.1 Hz, CH_3), 1.21 (t, 3H, J = 7.1 Hz, CH_3). ^{13}C NMR (101 MHz, $CDCl_3$) δ = 146.74–146.50 (m), 146.21 (d, J = 6.3 Hz, Car), 144.34–144.07 (m), 141.51–141.11 (m), 138.97–138.33 (m), 136.23–135.81 (m), 129.23 (s, 2 CHar), 118.77 (d, J = 0.4 Hz, CHar), 113.32 (d, 2 CHar), 111.40–111.22 (m, Car), 63.52 (d, J = 7.0 Hz, OCH_2), 62.36 (d, J = 7.4 Hz, OCH_2), 50.45 (d, J = 157.0 Hz, CHP), 24.28 (d, J = 6.9 Hz, $ArCH_2$), 16.43, 16.38, 16.35 and 16.29 (2 CH_3). ^{19}F NMR (377 MHz, $CDCl_3$) δ = −142.97 (dd, 2F, J = 22.5, 8.0 Hz), −155.98 (t, 1F, J = 20.9 Hz), −162.42 to −162.56 (m, 2F). ^{31}P NMR (162 MHz, $CDCl_3$) δ = 23.45 (s). HRMS (ESI^+) calcd. for $C_{18}H_{20}F_5NO_3P$ $([M+H]^+$): 424.1101, found: 424.1105.

*2.4.18. Diethyl (1-((4-chlorophenyl)amino)-2-(perfluorophenyl)ethyl)phosphonate (**1r**)*

Pale yellow solid (85 mg, 39%): ^1H NMR (400 MHz, $CDCl_3$) δ = 7.06–7.01 (m, 2H, 2 CHar), 6.48–6.44 (m, 2H, 2 CHar), 4.17–3.89 (m, 5H, 2 OCH_2, CH), 3.85–3.81 (m, 1H, NH), 3.26–3.20 (m, 2H, $ArCH_2$), 1.31 (t, 3H, J = 7.1 Hz, CH_3), 1.22 (t, 3H, J = 7.1 Hz, CH_3). ^{13}C NMR (101 MHz, $CDCl_3$) δ = 146.82–146.54 (m), 145.00 (d, J = 6.1 Hz, Car), 144.38–144.10 (m), 141.83–141.15 (m), 139.08–138.40 (m) 136.32–135.97 (m), 129.15 (s, 2 CHar), 123.24 (s, Car), 114.38 (s, 2 CHar), 111.34–111.06 (m, Car), 63.62 (d, J = 7.0 Hz, OCH_2), 62.51 (d, J = 7.5 Hz, OCH_2), 50.67 (d, J = 157.2 H z, CHP), 24.18 (d, J = 7.4 Hz, $ArCH_2$), 16.53, 16.48, 16.42 and 16.37 (2 CH_3). ^{19}F NMR (377 MHz, $CDCl_3$) δ = −142. 98 (dd, 2F, J = 22.5, 8.0 Hz), −155.48 (t, 1F, J = 20.9 Hz), −162.12 to −162.26 (m, 2F). ^{31}P NMR (162 MHz, $CDCl_3$) δ = 23.02 (s). HRMS (ESI^+) calcd. for $C_{18}H_{19}ClF_5NO_3P$ $([M+H]^+$): 458.0714, found: 458.0711.

*2.4.19. Diethyl (2-(perfluorophenyl)-1-(o-tolylamino)ethyl) phosphonate (**1s**)*

Pale yellow solid (42 mg, 20%): ^1H NMR (400 MHz, $CDCl_3$) δ = 7.02–6.99 (m, 2H, 2 CHar), 6.62 (t, 1H, J = 7.4 Hz, CHar), 6.50 (d, 1H, J = 8.5 Hz, CHar), 4.17–3.93 (m, 5H, 2 OCH_2, CH), 3.74 (s, 1H, NH), 3.30–3.11 (m, 2H, $ArCH_2$), 2.14 (s, 3H, $ArCH_3$) 1.29 (t, 3H, J = 7.1 Hz, CH_3), 1.20 (t, 3H, J = 7.1 Hz, CH_3). ^{13}C NMR (101 MHz, $CDCl_3$) δ = 14 6.96–146.52 (m), 144.50–144.26 (m), 144.17 (d, J = 4.7 Hz, Car), 141.67–141.19 (m), 139.03–138.43 (m), 136.33–135.98 (m), 130.57 (s, CHar), 127.00 (s, CHar), 122.57 (s, Car), 118.26 (s, CHar), 111.52–111.28 (m, Car), 110.37 (s, CHar), 63.42 (d, J = 7.0 Hz, OCH_2), 62.50 (d, J = 7.3 Hz, OCH_2), 50.12 (d, J = 155.6 Hz, CHP), 24.49 (d, J = 7.1 Hz, CH_2), 17.35 (s, $ArCH_3$), 16.50, 16.44 and 16.39 (2 CH_3). ^{19}F NMR (377 MHz, $CDCl_3$) δ = −142.80 (dd, 2F, J = 22.6, 8.0 Hz), −155.94 (t, 1F, J = 20.9 Hz), −162.40 to −162.47 (m, 2F).

^{31}P NMR (162 MHz, $CDCl_3$) δ = 23.59 (s). HRMS (ESI^+) calcd. for $C_{19}H_{21}F_5NO_3P$ ($[M+H]^+$): 438.1257, found: 438.1258.

2.4.20. Diethyl (2-(perfluorophenyl)-1-(m-tolylamino)ethyl) phosphonate (**1t**)

Pale yellow oil (69 mg, 33%): ^{1}H NMR (400 MHz, $CDCl_3$) δ = 6.96 (t, 1H, J = 7.6 Hz, CHar), 6.49 (d, 1H, J = 7.5 Hz, CHar), 6.34 (m, 2H, 2 CHar), 4.19–3.99 (m, 5H, 2 OCH_2, CH), 3.77 (d, 1H, J = 10.7 Hz, NH), 3.25–3.06 (m, 2H, $ArCH_2$), 2.20 (s, 3H, $ArCH_3$), 1.30 (t, 3H, J = 7.1 Hz, CH_3), 1.21 (t, 3H, J = 7.1 Hz, CH_3). ^{13}C NMR (101 MHz, $CDCl_3$) δ = 147.01–146.59 (m), 146.29 (d, J = 6.7 Hz, Car), 144.65–144.16 (m), 141.02–139.17 (m), 139.15(s, Car), 138.41–136.40 (m), 136.40–135.94 (m), 129.18 (s, CHar), 119.75 (s, CHar), 114.21 (s, CHar), 111.74–111.23 (m, Car), 110.56 (s, CHar), 63.63 (d, J = 7.0 Hz, OCH_2), 62.45 (d, J = 7.4 Hz, OCH_2), 50.48 (d, J = 157.0 Hz, CHP), 24.40 (d, J = 7.4 Hz, $ArCH_2$), 21.52 (s, $ArCH_3$), 16.55, 16.50, 16.46 and 16.40 (2 CH_3) ppm. ^{19}F NMR (377 MHz, $CDCl_3$) δ = −142.97 (dd, 2F, J = 22.6, 8.1 Hz), −156.21 (t, 1F, J = 20.8 Hz), −162.62to −162.76 (m, 2F). ^{31}P NMR (162 MHz, $CDCl_3$) δ = 23.50 (s). HRMS (ESI^+) calcd. for $C_{19}H_{22}F_5NO_3P$ ($[M+H]^+$): 438.1257, found: 438.1259.

2.4.21. Diethyl (2-(perfluorophenyl)-1-(p-tolylamino)ethyl) phosphonate (**1u**)

Pale yellow solid (63 mg, 30%): ^{1}H NMR (400 MHz, $CDCl_3$) δ = 6.89 (d, 2H, J = 8.0 Hz, 2 CHar), 6.45 (d, 2H, J = 8.4 Hz, 2 CHar), 4.17–3.94 (m, 5H, 2 OCH_2, CH), 3.67 (dd, 1H, J = 11.0, 4.1 Hz, NH), 3.24–3.05 (m, 2H, $ArCH_2$), 2.18 (s, 3H, $ArCH_3$), 1.29 (t, 3H, J = 7.1 Hz, CH_3), 1.21 (t, 3H, J = 6.9 Hz, CH_3). ^{13}C NMR (101 MHz, $CDCl_3$) δ = 146.88–146.59 (m), 144.46–144.06 (m), 143.96 (d, J = 6.5 Hz, Car), 141.19–141.05 (m), 139.05–138.35 (m), 136.40–135.92 (m), 129.78 (s, 2 CHar), 128.13 (s, Car), 113.55 (s, 2 CHar), 111.63–111.41 (m, Car), 63.59 (d, J = 7.0 Hz, OCH_2), 62.39 (d, J = 7.4 Hz, OCH_2), 50.90 (d, J = 156.8 Hz, CHP), 24.36 (d, J = 7.6 Hz, $ArCH_2$), 20.38 (s, $ArCH_3$), 16.55, 16.50, 16.44 and 16.38 (2 CH_3). ^{19}F NMR (377 MHz, $CDCl_3$) δ = −142.93 (dd, 2F, J = 22.8, 8.1 Hz), −156.21 (t, 1F, J = 20.9 Hz), −162.53 to −162.66 (m, 2F). ^{31}P NMR (162 MHz, $CDCl_3$) δ = 23.65 (s). HRMS (ESI^+) calcd. for $C_{19}H_{22}F_5NO_3P$ ($[M+H]^+$): 438.1257, found: 438.1255.

2.5. Cyclic α-aminophosphonates

2.5.1. Diethyl (4,6-difluoro-1-(phenyl)indolin-2-yl)phosphonate (**5g**)

Yellow oil (44 mg, 21%): ^{1}H NMR (400 MHz, $CD_3C(O)CD_3$) δ = 7.50 (d, J = 8.0 Hz, 2H, 2 CHar), 7.42 (t, J = 7.9 Hz, 2H, 2 CHar), 7.20 (t, J = 7.3 Hz, 1H, CHar), 6.37 (td, J = 9.5, 2.0 Hz, 1H, CHar), 6.25 (dd, J = 10.0, 1.9 Hz, 1H, CHar), 4.81 (dd, J = 11.2, 5.9 Hz, 1H, CHar), 4.03–3.96 (m, 5H, 2 OCH_2, CH), 3.64–3.52 (m, 1H, $ArCH_2$), 3.40–3.30 (m, 1H, $ArCH_2$), 1.14, 1.12, 1.10 and 1.08 (2 CH_3). ^{13}C NMR (101 MHz, $CDCl_3$) δ = 164.03 (dd, J = 243.6 Hz, 13.1 Hz, Car), 160.20 (dd, J = 245.8 Hz, 15.3 Hz, Car), 152.34–152.04 (m, Car), 143.63 (s, Car), 129.55 (s, 2 CHar), 125.13 (s, CHar), 123.20 (s, 2 CHar), 110.49–110.19 (m, Car), 95.23–94.45 (m, 2 CHar), 62.84 (d, J = 6.8 Hz, OCH_2), 62.56 (d, J = 7.2 Hz, OCH_2), 62.32 (d, J = 167.4 Hz, CHP), 27.38 (s, $ArCH_2$), 16.47, 16.41, 16.39, and 16.33 (2 CH_3). ^{19}F NMR (377 MHz, $CD_3C(O)CD_3$) δ = −112.99 (d, J = 6.5 Hz, 1F), −117.67 (d, J = 6.6 Hz, 1F). ^{31}P NMR (162 MHz, $CD_3C(O)CD_3$) δ = 21.93 (s). HRMS (ESI^+) calcd. for $C_{18}H_{21}F_2NO_3P$ ($[M+H]^+$): 368.1227, found: 368.1226.

2.5.2. Diethyl (4,6-difluoro-1-(p-chlorophenyl)indolin-2-yl) phosphonate (**5h**)

Colorless oil (40 mg, 17%): ^{1}H NMR (400 MHz, $CD_3C(O)CD_3$) δ = 7.56–7.53 (m, 2H, 2CHar), 7.44–7.40 (m, 2H, 2 CHar), 6.40–6.33 (m, 2H, 2 CHar), 4.79 (dd, J = 11.1, 5.4 Hz, 1H, CH), 4.05–3.95 (m, 4H, 2 OCH_2), 3.65–3.52 (m, 1H, $ArCH_2$), 3.39–3.28 (m, 1H, $ArCH_2$), 1.17 (t, J = 7.0 Hz, 3H, CH_3), 1.10 (t, J = 7.0 Hz, 3H, CH_3). ^{13}C NMR (101 MHz, $CDCl_3$) δ = 163.56 (dd, J = 244.2, 13.0 Hz, Car), 159.01 (dd, J = 246.3, 15.2 Hz, Car), 151.72–151.42 (m, Car), 142.34 (s, Car), 130.13 (s, Car), 129.59 (s, 2 CHar), 124.20 (s, 2 CHar), 110.76–110.47 (m, Car), 95.67–94.77 (m, 2 CHar), 63.06 (d, J = 6.9 Hz, OCH_2), 62.58 (d, J = 7.1 Hz, OCH_2), 62.55 (d, J = 167.6 Hz, CHP), 27.39 (s, $ArCH_2$), 16.50, 16.44 and 16.38 (2 CH_3). ^{19}F NMR (377 MHz, $CD_3C(O)CD_3$) δ = −112.72 (d, J = 6.5 Hz, 1F), −117.37 (d, J = 6.7 Hz, 1F). ^{31}P NMR (162 MHz, $CD_3C(O)CD_3$) δ = 21.65 (s). HRMS (ESI^+) calcd. for $C_{18}H_{20}ClF_2NO_3P$ ($[M+H]^+$): 402.0837, found: 402.0837.

2.5.3. Diethyl (4,6-difluoro-1-(m-tolyl)indolin-2-yl) phosphonate (**5j**)

Yellow oil (22 mg, 10%): ^{1}H NMR (400 MHz, $CD_3C(O)CD_3$) δ = 7.33 (s, 1H, CHar), 7.30–7.28 (m, 2H, 2 CHar), 7.04–7.02 (m, 1H, CHar), 6.34–6.29 (m, 1H, CHar), 6.23 (dd, J = 10.1, 2.1 Hz, 1H, CHar), 4.79 (ddd, J = 11.2, 6.0, 0.5 Hz, 1H, CH), 4.05–3.84 (m, 4H, 2 OCH_2), 3.59–3.51 (m, 1H, $ArCH_2$), 3.39–3.28 (m, 1H, $ArCH_2$), 2.35 (s, 3H, $ArCH_3$), 1.13–1.09 (m, 6H, CH_3). ^{13}C NMR (101 MHz, $CDCl_3$) δ = 163.55 (dd, J = 243.5 Hz, 12.9 Hz, Car), 158.98 (dd, J = 245.4 Hz, 15.2 Hz, Car), 152.55–152.24 (m, Car), 143.64 (s, Car), 139.47 (s, Car), 129.35 (s, CHar), 126.00 (s, CHar), 123.86 (s, CHar), 120.33 (s, CHar), 110.45–110.14 (m, Car), 95.06–94.55 (m, 2 CHar), 62.81 (d, J = 6.9 Hz, OCH_2), 62.56 (d, J = 7.1 Hz, OCH_2), 62.35 (d, J = 167.7 Hz, CHP), 27.39 (s, $ArCH_2$), 21.62 (s, $ArCH_3$), 16.46, 16.40 and 16.35 (2 CH_3). ^{19}F NMR (377 MHz, $CD_3C(O)CD_3$) δ = 64.46 (d, J = 6.6 Hz, 1F), 59.73 (d, J = 6.5 Hz, 1F). ^{31}P NMR (162 MHz, $CD_3C(O)CD_3$) δ 21.99 (s). HRMS (ESI^+) calcd. for $C_{19}H_{23}F_2NO_3P$ ($[M+H]^+$): 382.1384, found: 382.1381.

2.5.4. Diethyl (4,5,6,7-tetrafluoro-1-(phenyl)indolin-2-yl) phosphonate (**5r**)

Green oil (7.5 mg, 4%): ^{1}H NMR (400 MHz, $CD_3C(O)CD_3$) δ = 7.26–7.20 (m, 4H, 4 CHar), 6.99 (bt, J = 7.2 Hz, 1H, CHar), 4.42–4.36 (m, 1H, CH), 4.07–3.87 (m, 4H, 2 OCH_2), 3.80–3.64 (m, 1H, $ArCH_2$), 3.21 (bt, J = 17.9 Hz, 1H, $ArCH_2$), 1.15 (t, J = 7.1 Hz, 3H, CH_3), 1.02 (t, J = 7.0 Hz, 3H, CH_3). ^{13}C NMR (101 MHz, $CDCl_3$) δ = 145.48–145.45 (m, Car), 144.91–144.69 (m), 142.51–142.19 (m), 137.72–137.72 (m), 135.27–134.85 (m), 131.36–131.11 (m, Car), 129.22 (s, 2 CHar), 124.25 (s, CHar), 120.24 (s, 2 CHar), 114.71–114.43 (m, Car), 65.62 (d, J = 172.3 Hz, CH), 63.52 (d, J = 7.2 Hz, OCH_2), 62.98 (d, J = 7.2 Hz, OCH_2), 28.77

(s, $ArCH_2$), 16.60, 16.54 and 16.49 (2 CH_3). ^{19}F NMR (377 MHz, $CD_3C(O)CD_3$) δ = −145.39 (dd, *J* = 21.6, 14.2 Hz, 1F), −150.35 to −150.45 (m, 1F), −160.07 (bt, *J* = 19.1 Hz, 1F), −168.57 (t, *J* = 20.0 Hz, 1F). ^{31}P NMR (162 MHz, $CD_3C(O)CD_3$) *δ* = 21.21 (s). HRMS (ESI^+) calcd. for $C_{18}H_{19}F_4NO_3P$ ($[M+H]^+$): 404.1039, found: 404.1035.

2.5.5. Diethyl (4,5,6,7-tetrafluoro-1-(p-chlorophenyl)indolin-2-yl)phosphonate (**5t**)

Yellow oil (26 mg, 12%): ^1H NMR (600 MHz, $CD_3C(O)CD_3$) *δ* = 7.44–7.42 (m, 2H, 2 CHar), 7.36–7.34 (m, 2H, 2 CHar), 4.57 (ddd, *J* = 10.9, 4.1, 3.0 Hz, 1H, CH), 4.19–4.00 (m, 4H, OCH_2), 3.87 (ddd, *J* = 28.7, 17.0, 11.2 Hz, 1H, $ArCH_2$), 3.37–3.31 (bt, 1H, *J* = 17.9 Hz, $ArCH_2$), 1.29 (t, *J* = 7.0 Hz, 3H, CH_3), 1.13 (t, *J* = 7.0 Hz, 3H, CH_3). ^{13}C NMR (101 MHz, $CDCl_3$) *δ* = 144.88–144.76 (m), 144.0 (d, *J* = 2.8 Hz, Car), 142.3–142.4 (m), 140.0–139.7 (m), 137.9–137.3 (m), 135.3–135 (m), 130.9–130.7 (m, Car), 129.4 (s, Car), 129.2 (s, 2CHar), 121.63 (s, 2 CHar), 114.52 (d, *J* = 18.8 Hz, Car), 65.60 (d, *J* = 172.4 Hz, CHP), 63.6 (d, *J* = 7.1 Hz, OCH_2), 63.00 (d, *J* = 7.1 Hz, OCH_2), 28.8 (s, $ArCH_2$), 16.59 (d, *J* = 6.0 Hz, CH_3), 16.47 (d, *J* = 6.0 Hz, CH_3). ^{19}F NMR (565 MHz, $CD_3C(O)CD_3$) δ = −145.13 (dd, *J* = 21.6, 14.1 Hz, 1F), −149.92 (dd, *J* = 19.4, 14.3 Hz, 1F), −159.72 (t, *J* = 19.2 Hz, 1F), −167.94 (t, *J* = 20.0 Hz, 1F). ^{31}P NMR (243 MHz, $CD_3C(O)CD_3$) *δ* = 21.01 (s). HRMS (ESI^+) calcd. for $C_{18}H_{18}ClF_4NO_3P$ ($[M+H]^+$): 438.0649, found: 438.0650.

2.5.6. Diethyl (4,5,6,7-tetrafluoro-1-(m-tolyl)indolin-2-yl) phosphonate (**5u**)

Yellow oil (14 mg, 7%): ^1H NMR (400 MHz, $CD_3C(O)CD_3$) *δ* = 7.23–7.18 (m, 3H, 3 CHar), 6.95–6.90 (m, 1H, CHar), 4.50 (ddd, *J* = 10.9, 4.4, 3.1 Hz, 1H, CH), 4.14–4.11 (m, 4H, 2 OCH_2), 3.85 (ddd, *J* = 28.0, 15.3, 10.7 Hz, 1H, $ArCH_2$), 3.32 (bt, *J* = 18.3 Hz, 1H, $ArCH_2$), 2.31 (s, 3H, CH_3), 1.28 (t, *J* = 7.0 Hz, 3H, CH_3), 1.15 (t, *J* = 7.0 Hz, 3H, CH_3). ^{13}C NMR (101 MHz, $CDCl_3$) *δ* = 145.6 (m), 144.7 (d, *J* = 12.0 Hz, Car), 142.5–142.4 (m), 140.2–139.8 (m), 139.2 (s, Car), 137.8–137.6 (m), 135.2–134.9 (m), 131.6–131.3 (m, Car), 129.0 (s, CHar), 125.1 (s, CHar), 120.9 (s, CHar), 117.3 (s, CHar), 114.6 (d, *J* = 16.3 Hz, Car), 65.6 (d, *J* = 172.3 Hz, CHP), 63.5 (d, *J* = 7.1 Hz, OCH_2), 63.0 (d, *J* = 7.2 Hz, OCH_2), 28.75 (s, $ArCH_2$), 21.66 (s, $ArCH_3$), 16.58 (d, *J* = 5.3 Hz, CH_3), 16.53 (d, *J* = 5.2 Hz, CH_3). ^{19}F NMR (565 MHz, $CD_3C(O)CD_3$) δ = −145.43 (dd, *J* = 21.6, 14.2 Hz), −150.42 (dd, *J* = 18.9, 14.7 Hz), −160.04 (t, *J* = 19.2 Hz), −168.60 to −168.67 (m). ^{31}P NMR (243 MHz, $CD_3C(O)CD_3$) *δ* = 21.25 (s). HRMS (ESI^+) calcd. for $C_{19}H_{21}F_4NO_3P$ ($[M+H]^+$): 418.1195, found: 418.1194.

2.6. X-ray diffraction

Reflection intensities for **1a-1u** were measured on Xcalibur diffractometer (Eos detector) equipped with a graphite monochromator and MoKα radiation (λ = 0.71073 Å). Data reduction and analysis were carried out with the CrysAlisPro software (CrysAlisPro, version 171.38.46, 2015). In all single-crystal experiments, except for **1o**, the temperature of the crystals was controlled with an Oxford Instruments Cryosystem cold nitrogen-gas blower. The crystals of **1j**, **1L** and **1s** were found to be excessively non-merohedrally twinned. The reflections of the two twin components were separated using the CrysAlisPro.

In **1j** component 2 rotated about 6.26° around [0.54 0.31 −0.78] direct lattice direction, in **1L** it is rotated by about 2.85° around [0.85 0.04 0.53] the direct lattice direction and in **1s** it is rotated by about 1.91° around [−0.86 0.50 −0.12] direct lattice direction. The structures were solved by direct methods using SHELXS (Sheldrick, 2015) and refined by the full-matrix least-squares techniques with SHELXL (Sheldrick, 2015). All heavy atoms were refined anisotropically. The hydrogen atoms bound to C atoms were placed at calculated positions and refined using a riding model, and their isotropic displacement parameters were given a value 20% higher than the isotropic equivalent for the atom to which the H atoms were attached (for methyl hydrogen atoms this value has been increased to 50%). The positions of the amine H atoms were located reliably on difference Fourier maps and their position and displacement parameters were refined.

In **1d**, one of the ethyl groups are split over two positions with final occupation factors of 0.5. In **1g**, terminal carbon atom of the ethyl group is split up into two positions with site occupation factors refined to 0.70 and 0.30. In **1j** the disordered regions include a methyl group in the aniline ring that could be split into two positions with site occupancy factors refined to 0.75 and 0.25. The ethyl group is also disordered over two sites. The occupancies for the two positions were refined to 0.6 and 0.4. In **1m** the disordered regions include one ethyl group of molecule 1 and fluorinated phenyl ring of molecule 2 that both could be split over two positions. The site occupancy factors for both cases were refined to 0.5. In **1u**, the methyl group attached to aniline moiety displays dynamic disorder with two alternative positions of methyl hydrogen atoms. Where necessary, restraints for the 1,2- and 1,3-distances as well as the ADP restraint (SIMU) and rigid-bond restraint (DELU) were applied. Graphical images were produced in Xseed (Barbour, 2001) using Pov-Ray (POV-RayTM for Windows, version 3.6, Persistence of Vision Raytracer Pty Ltd, 2004) and Mercury (Bruno et al., 2002) programs. Hirshfeld surfaces have been calculated using CrystalExplorer (Wolff et al., 2013) in order to identify the important intermolecular interactions within the crystal structures investigated.

2.7. Computational methods

Conformations of the studied compounds have been subjected to cluster analysis based on RMSD matrix between different structures. Agglomerative hierarchical clustering (Szekely and Rizzo, 2005) and k-medoids algorithm (Park and Jun, 2009) have been used. In the latter case dimensionality reduction with principal component analysis (Abdi and Williams, 2010) was performed to graphically represent the resulting clusters of conformers.

Based on the cluster analysis the representative molecules have been selected and subjected to quantum chemical calculations in order to explain if the observed in crystals conformational diversity is the result of conformational preferences of isolated molecules or stems from crystal packing. Three different DFT potentials namely B3LYP (Becke, 1993; Lee et al., 1988), M06 (Zhao and Truhlar, 2008), and wB97XD (Chai and Head-Gordon, 2008) with basis sets 6-31G(d) (Francl

et al., 1982; Hariharan and Pople, 1973) and 6-311 + + G(d,p) (Clark et al., 1983; Krishnan et al., 1980) have been utilized to assess energy differences between three main conformers observed in the crystal structures, for which bond distances and valence angles have been optimized. The attempt to calculate energies for these conformers at MP2 level of theory (Møller and Plesset, 1934) failed due to limitations on disk space and computer time.

3. Results and discussion

3.1. Synthesis

3.1.1. Synthesis of fluorinated aldehydes *3a-3d*

A synthetic route based on commercially available fluorinated phenylacetic acids was planned for preparation of fluorinated aldehyde precursors **3a-d** (Scheme 1). The first step consisted in reduction of the fluorinated phenylacetic acid carboxylic group by $LiAlH_4$ in refluxing diethyl ether (Scheme 1). The reaction proceeded efficiently with complete conversion of the acids into corresponding alcohols **4a-d** within short reaction time (generally in 1 h) in almost quantitative yields (Table 1). It is important to note that alcohol **4a** has already been synthesized from (4-fluorophenyl)acetic acid using $LiAlH_4$ as reducing agent in THF (Kawasaki et al., 2001) In our case, we observed a beneficial quantitative yield when a larger quantity of hydride was used (86% vs. 99% yield).

Several oxidizing reagents were evaluated for the obtained alcohols oxidation. Some procedures were already described for transformation of alcohols **4a** and **4d**. Thus, PCC (Jang et al., 2011), Dess-Martin periodinane (DMP) (Kolonko and Reich, 2008), and $Na_2Cr_2O_7$š$2H_2O$ (Rao and Filler, 1974) were evaluated for the preparation of **3a** or **3d**. Among these reagents, only freshly synthesized Dess-Martin periodinane in dichloromethane afforded 2-(perfluorophenyl)ethanal **3d** in 54% yield (Table 1). Aldehyde **3d** had a limited stability and acetic acid issued from DMP reagent had to be carefully removed prior purification of the aldehyde by chromatography on silica gel. Once aldehyde **3d** was isolated, it had to be promptly engaged in the synthesis of α-aminophosphonates. The other aldehydes **3a-c** were prepared in the same manner in yields ranging from 57% to 62% (Table 1). Aldehydes **3a** and **3c** were found to be more stable; their complete degradation was achieved in 7 days of storage at −24 °C under a nitrogen atmosphere whereas only 3 days were sufficient for decomposition of the aldehyde **3b**. Compounds **3a-d** differ by the number and the position of fluorine atoms in the aromatic ring, and both parameters have a decisive influence on this chemical instability.

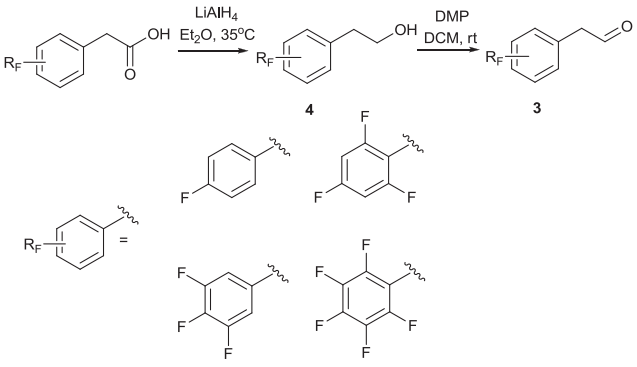

Scheme 1 Reduction of the carboxylic group of fluorinated phenylacetic acids to alcohols **4** and oxidation by Dess-Martin periodinane to corresponding aldehydes **3**.

3.1.2. Synthesis of α-aminophosphonates *1a-1u*

At first intention, the three-component Kabachnik-Fields reaction (Cherkasov and Galkin, 1998) was planned to produce fluorinated α-aminophosphonates **1**. Mixing together aniline, 2-(perfluorophenyl)ethanal (**3d**) and diethyl phosphite in refluxing toluene overnight unfortunately gave a complex mixture, and α-aminophosphonate **1q** could not be isolated. To circumvent this problem, it was preferred to accomplish a one-pot sequential reaction as depicted in Scheme 2, firstly preparing the imine derivative, and secondly by adding diethyl phosphite once the imine was formed. This approach was first tested for preparation of α-aminophosphonate **1q**. The imine was successfully obtained by mixing equimolar ratio of 2-(perfluorophenyl)ethanal (**3d**) with aniline in refluxing toluene for 4 h with concomitant removal of water using a Dean-Stark apparatus. Thereafter, these favorable conditions were generalized to the *in situ* preparation of other imines. For the second step of the sequence, several reaction conditions were evaluated. The best ones were the nucleophilic addition of diethyl phosphite (2 equiv.) to imine in the presence of sodium hydride (2 equiv.). After heating in refluxing toluene during 18 h, aminophosphonate **1q** was isolated in 49% yield. A larger excess of diethyl phosphite and base did not change significantly the yield. Therefore, ratio in diethyl phosphite/base of 2:2 was adopted for preparation of twenty-one fluorinated α-aminophosphonates **1**, while adapting the reaction time (Table 2). In these conditions, we noticed the formation of a minor impurity consisting in 2-indolinylphosphonates **5** (Fig. 2).

The formation of these cyclic α-aminophosphonates **5** was not so surprising. Indeed, phenyl groups substituted at least by one fluorine atom and one or more electron withdrawing groups can undergo S_NAr reactions with diverse nucleophilies (Ajenjo et al., 2016; Gutsche et al., 2016; Korb et al., 2016). Obviously, only aminophosphonates issued from aldehyde **3b** and **3d**, exhibiting an electronically depleted aromatic group, and possessing a fluorine atom in *ortho* position of the phosphonoalkyl substituent could be transformed into S_NAr reaction products. Indolinylphosphonates **5g**, **5h**, **5j**, **5r**, **5t** and **5u** were respectively isolated in yields ranging from 4% to 21%.

3.2. Structural studies

3.2.1. X-ray crystal structures

Single-crystal X-ray analysis was carried out on a series of α-aminophosphonates **1a** to **1u** but not for **1i**, **1n**, **1p** and **1t**. To the best of our knowledge, these crystal structures have not been reported thus far.

Single crystals of **1a** through **1u** were obtained by slow evaporation from toluene solutions. Only **1d** crystallizes with toluene in ratio 2:1 (**1d**:tol). Details of the X-ray diffraction data collections are given in Tables S1–S3 in the ESI.

Table 1 Substrate scope of primary alcohols and aldehydes.

Alcohol	R_F	Yield (%)	Aldehyde	Yield (%)
4a	4-F	99	**3a**	57
4b	2,4,6-F_3	100	**3b**	62
4c	3,4,5-F_3	98	**3c**	57
4d	2,3,4,5,6-F_5	96	**3d**	54

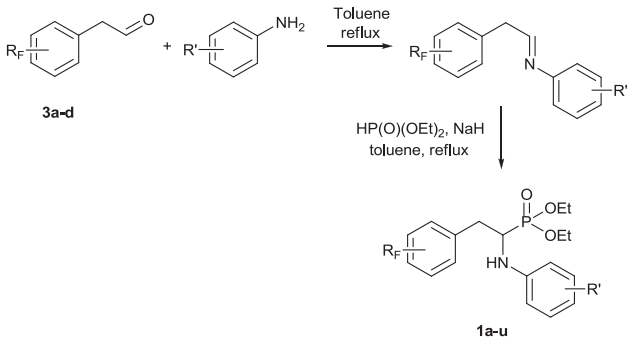

Scheme 2 Synthesis of **1a-u**.

All the molecules in the series **1a** through **1u** are chiral, however, they are not enantiomerically pure. During the synthesis procedure the racemic mixtures were obtained. Crystallization thus yielded single crystals containing both enantiomers. **1b**, **1c**, **1d**, **1e**, **1f**, **1g**, **1j**, **1k**, **1o**, **1s** and **1u** crystallized with a single molecule in the asymmetric unit while **1a**, **1h**, **1L**, **1m**, **1q** and **1r** crystallized with two molecules in the asymmetric unit. All crystals were chosen such that the *R* enantiomer constitutes the asymmetric unit.

The α-aminophosphonates generally consist of two moieties: an aliphatic diethyl phosphonate moiety and the rest of molecule which includes a stereogenic centre and two aromatic rings. In the crystals the aliphatic diethyl phosphonate chain (C^3_{sp}-C^3_{sp}-O-P) can adopt one of three conformations, either an *antiperiplanar* (*ap*), *anticlinal* (−*ac* or +*ac*) or *synclinal* (−*sc* or +*sc*) conformation. For the two aliphatic diethyl phosphonate chains only four sets of the conformational combinations are observed: *ap-ap*, *ac-ac*, *ap-ac* and *ap-sc*. While the aliphatic moieties of molecule are common across the series, the remaining groups are fundamentally different in terms of their chemistry. These differences mainly include the num-

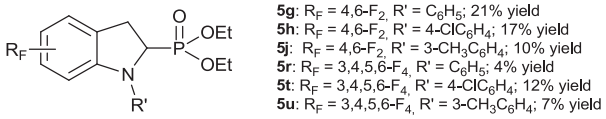

Fig. 2 Isolated indolin-2-yl phosphonates **5**.

Table 2 Reaction times of second step and yields for **1a** to **1u**. Conformations adopted in crystals.

Product	R_F	R′	Time of 2nd step (h)	Yield isolated (%)	Conformation in crystal
1a	4-F	H	18	21	A
1b	4-F	4-Cl	18	20	A
1c	4-F	2-CH_3	4	20	A
1d	4-F	3-CH_3	4	25	A
1e	4-F	4-CH_3	18	28	B
1f	4-F	4-NO_2	4	27	A
1g	2,4,6-F_3	H	18	22	B
1h	2,4,6-F_3	4-Cl	18	27	B
1i	2,4,6-F_3	2-CH_3	3	35	–[a]
1j	2,4,6-F_3	3-CH_3	3	15	A
1k	3,4,5-F_3	H	18	22	B
1l	3,4,5-F_3	4-Cl	18	22	A
1m	3,4,5-F_3	2-CH_3	4	27	A
1n	3,4,5-F_3	3-CH_3	4	15	–[a]
1o	3,4,5-F_3	4-CH_3	18	20	B
1p	3,4,5-F_3	4-NO_2	4	20	–[a]
1q	2,3,4,5,6-F_5	H	18	49	C
1r	2,3,4,5,6-F_5	4-Cl	18	39	A
1s	2,3,4,5,6-F_5	2-CH_3	18	20	C
1t	2,3,4,5,6-F_5	3-CH_3	18	33	–[a]
1u	2,3,4,5,6-F_5	4-CH_3	18	30	C

[a] Oil.

ber of fluorine atoms in one aromatic ring as well as various substitutions of the aniline moiety.

Regardless of the chemical modifications implemented in both aromatic rings, the molecules in the crystals adopt one of the three conformations that can be described by a set of two torsion angles C^2_{sp}-N-C^3_{sp}-C^3_{sp} and C^2_{sp}-C^3_{sp}-C^3_{sp}-N as well as by the dihedral angle of two aromatic rings (for the definition see ESI Fig. S147). All of the angles describe the mutual orientation of the aromatic rings. The results are summarized in Table 3. The absolute values of the torsion angles for C^2_{sp}-N-C^3_{sp}-C^3_{sp} are in the range 99–137° and for C^2_{sp}-C^3_{sp}-C^3_{sp}-N are in the range 47–75°, corresponding to the *ac* and *sc* conformation, respectively. This combination represents the A conformer (Fig. 3). With regard to this combination (*ac* and *sc*), the dihedral angle adopts values in the range 43–83°. In contrast, conformers B and C adopt an *ap* and *sc* combination with the corresponding values *ca*. 162° and 65° for B, and 82 and 163° for C, respectively. However, in conformer B the aromatic rings are oriented almost perpendicular to each other and the mean value of the dihedral angle is 86° while in conformer C the aromatic rings are roughly parallel with a value of 13°. It would appear that conformer C is stabilized by intramolecular C—H···π interactions; however, the shortest H···π distances are over 3 Å and are thus beyond the cut-off limit accepted for this type of interaction (Desiraju and Steiner, 1999). It is interesting to note that there are two symmetry independent molecules in the crystal structure of **1 h** that simultaneously adopt two different conformations (A and B).

In all crystal structures investigated the principal directional interactions are the N—H···O hydrogen bonds that hold two enantiomers of opposite stereochemistry together around a centre of symmetry. This hydrogen bonding interactions produce acyclic motif that can be described by the graph set notation $R^2_2(10)$, as shown in Fig. 4. It appears in all the crystal structures investigated. Geometrical parameters describing intermolecular interactions are listed in Table S4 in the ESI.

We estimated the intermolecular contacts contributing to the Hirshfeld surfaces for all crystals investigated and the results of our analysis are shown in Fig. 5. The Hirshfeld surface analysis reveals a similar proportion of H···O contacts, representing O—H···O and C—H···O interactions, for each of molecules investigated ranging from 7 to 12%. The exception is **1f** for which the contact contribution increases to 27% and results from the introduction of the nitric group (oxygen atom containing group) to the aniline moiety. **1a** has the highest H···H interactions contribution (61%) while **1r** has the lowest (29%). This is evidence that van der Waals forces exert an important influence on the stabilization of the packing. The number of fluorine atoms increases in the aromatic ring from one in **1a-1f** to five in **1q-1u**, the proportion of H···F contacts simultaneously increases from 8 to 36% at the expense of H···H contacts. Patches of the molecular surfaces involved in the C—H···F interactions (**1a** and **1s**) are displayed in Fig. 6.

3.2.2. NMR studies

Structures of all α-aminophosphonates synthesized were studied using spectroscopic and spectrometric methods. ^{1}H NMR, ^{19}F NMR, ^{31}P NMR and ^{13}C NMR, as well as HRMS spectra were recorded for the compounds (see Experimental Section and ESI Figs. S9–S93, and Figs. S118–S138). For the purpose of investigating conformational preferences of the α-aminophosphonates in solution, more detailed NMR studies based on 2D experiments were performed for **1f**, **1o** and **1u**. These compounds were chosen because in the crystalline state their molecular structures represent three different conformations A, B and C. It is worth noticing that others α-aminophosphonates studied in this work adopted in crystals

Table 3 Values of the torsion angles and dihedral angle describing conformation of the molecules investigated.

		C^2_{sp}-N-C^3_{sp}-C^3_{sp} (°)	C^2_{sp}-C^3_{sp}-C^3_{sp}-N (°)	Dihedral angle (°)	Conformer
1a	*mol1*	137	−71	83	A
	mol2	137	−71	77	A
1b		132	−73	69	A
1c		120	−63	51	A
1d		134	−75	74	A
1e		162	−62	87	B
1f		116	−59	51	A
1g		159	−66	90	B
1h	*mol1*	−160	66	86	B
	mol2	135	−62	77	A
1j		102	−62	48	A
1k		169	−65	79	B
1l	*mol1*	131	−59	68	A
	mol2	99	−60	43	A
1m	*mol1*	124	−60	56	A
	mol2	−129	59/61	66/57	A
1o		159	−69	86	B
1q	*mol1*	86	−162	5	C
	mol2	−75	164	16	C
1r	*mol1*	102	−48	46	A
	mol2	99	−47	45	A
1s		83	−165	18	C
1u		85	−161	13	C

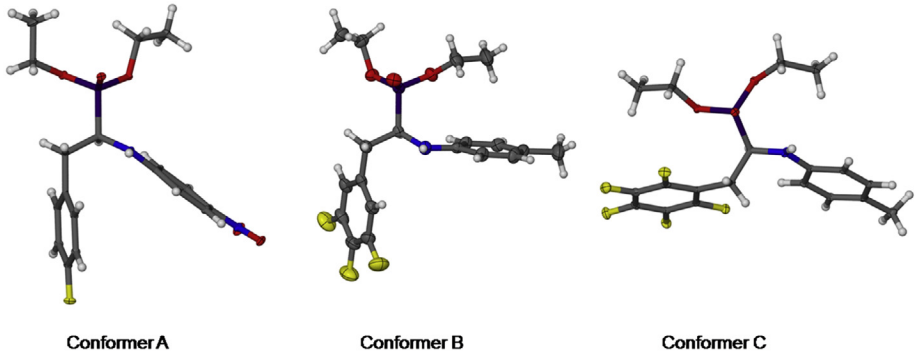

Fig. 3 The three possible conformers; the conformer A, B and C represented by **1f**, **1o** and **1u**, respectively. Ellipsoids are drawn at the 30% probability level, hydrogen atoms are represented by spheres of arbitrary radii.

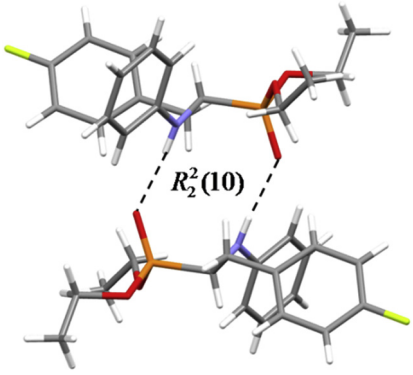

Fig. 4 Dimeric motif of N—H···O(=P) hydrogen bonds present in all crystals investigated.

one of the three conformations. The assignment of signals observed in the ^{1}H NMR spectra of the three compounds was based on proton chemical shift and 2D homonuclear H-H correlation (COSY) experiments. The results are summarized in Table 4. (For ^{1}H NMR, COSY and NOESY spectra see ESI Figs. S258–S266).

For the compounds **1f**, **1o** and **1u** also NOESY experiments were performed. Among the correlations observed in the NOESY spectrum of **1f** (Fig. 7) the strongest were of Ha′ with N<u>H</u>, and *C<u>H</u>, respectively. Strong correlation signals were also observed between Ha and both protons of the methylene group as well as between *C<u>H</u> and one proton of the OC<u>H</u>$_2$ group. Distinctively less intense correlations were detected between Ha and *C<u>H</u>, and N<u>H</u>, respectively. Almost the same intensity characterized correlation signal of N<u>H</u> with this proton of the methylene group to which chemical shift at δ = 2.97 ppm was assigned.

Analysis of the NOESY spectra of **1o** and 1**u** revealed that similar to the spectrum of **1f**, the strongest signals were observed for correlation between Ha′ and *C<u>H</u> protons. Signals resulted from correlations of Ha′ with N<u>H</u> were also strong, however contrary to the spectrum of **1f**, not as strong as the ones with *C<u>H</u>. The intensity of signals derived from correlations between Hb′ and ArC<u>H</u>$_3$ was also strong and comparable with this observed for correlation signal of Ha′ with N<u>H</u> protons. Correlation signals observed in the NOESY

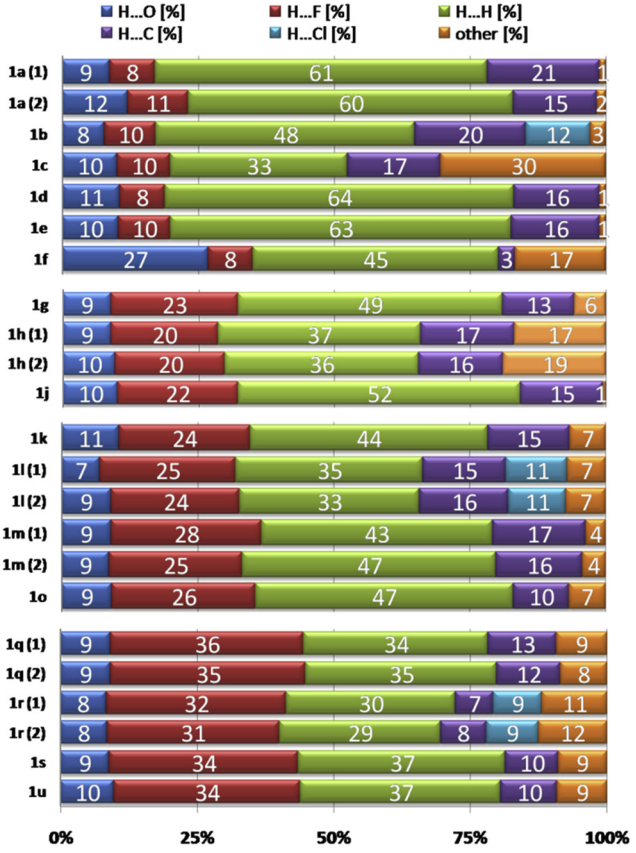

Fig. 5 Percentage contributions to the Hirshfeld surface area for the close intermolecular contacts for molecules in all crystals investigated.

spectrum of **1o** between Ha and the methylene group protons and with *C<u>H</u>, were weaker. A very weak signal resulted also from correlation of Ha′ and of *C<u>H</u> with one of the OC<u>H</u>$_2$ group protons. It is worth stressing that presence of the former signal is a unique feature of the **1o** NOESY spectrum; this kind of correlation was not detected in the spectra of **1f** neither **1u**. Interestingly in the spectrum of **1u** the signal showing presence of correlation between *C<u>H</u> and proton of the OC<u>H</u>$_2$ group was strong, while signals responsible for correlations of the *C<u>H</u> and N<u>H</u> protons with both methylene group protons were

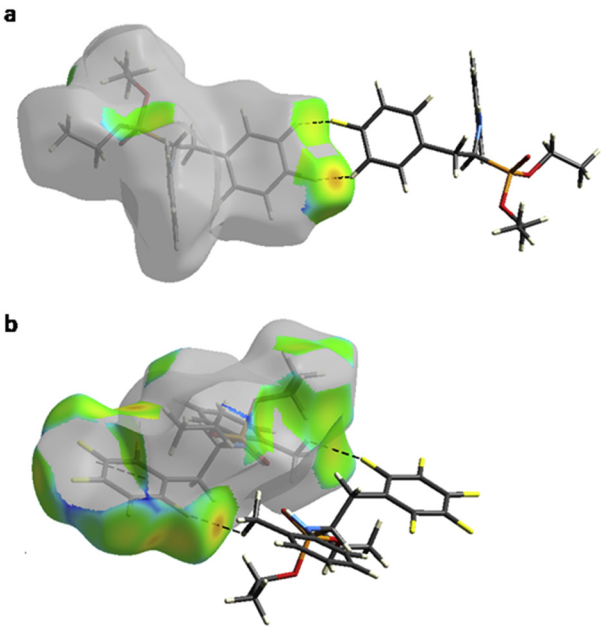

Fig. 6 The surface patches associated with H···F contacts reflect weak intermolecular C—H···F interactions in crystals **1a** (a) and **1s** (b).

weak. The weakest in the **1u** spectrum was the signal resulted from correlation between NH proton and this proton of the methylene group to which chemical shift at δ = 3.20 ppm was assigned.

Analysis of data obtained from 2D experiments performed for compounds **1f**, **1o** and **1u** revealed that the resulted COSY and NOESY spectra differ in the type and intensity of the correlation signals. Based on these data it can be concluded that in solution, like in solid state, the compounds investigated adopt different conformations. It is seems, however, that the conformations observed in solution are different from these adopted in the solid state and that the latter ones result from crystal packing.

3.2.3. Theoretical studies

Theoretical calculations were based on molecular geometries derived from crystals. In the first step an attempt to allocate molecules of seventeen compounds investigated to groups of a similar conformation was made. For this purpose cluster analysis based on RMSD matrix between different structures was performed. Fig. 8 presents the graphical two dimensional representation of the results for 3-medoid clustering of conformers observed in the crystal structures.

The three clusters were composed of molecules {**1a**, **1b**, **1c**, **1d**, **1f**, **1j**, **1L**, **1m**, **1r**} present in the crystals in the conformation A, molecules {**1e**, **1g**, **1h**, **1k**, **1o**} observed in the confor-

Table 4 ^{1}H chemical shifts (δ), and H,H (COSY) correlations observed in the NMR spectra of **1f**, **1o** and **1u**.

		1f		**1o**		**1u**
Proton	δ (ppm)	COSY	δ (ppm)	COSY	δ (ppm)	COSY
Ha (2H)	7.18	Hb	6.85	–	–	–
Hb (2H)	6.92	Ha	–	–	–	–
Ha′ (2H)	6.49	Hb′	6.47	Hb′	6.45	Hb′, $ArCH_3$
Hb′ (2H)	7.98	Ha′	6.95	Ha′, $ArCH_3$	6.90	Ha′, $ArCH_3$
ArCH′ (1H)	2.97	H″, *CH	2.88	H″, *CH	3.10	H″, *CH
ArCH″ (1H)	3.27	H′, *CH	3.14	H′, *CH	3.20	H′, *CH
*CH (1H)	4.01	H′, H″, NH	3.89	H′, H″, NH	4.01	H′, H″, NH
NH (1H)	5.20	*CH	3.66	*CH	3.67	*CH
2 OCH_2 (4H)	4.19–3.95	CH_3	4.12–3.94	CH_3	4.17–3.95	CH_3
$OCH_2C\underline{H}_3$ (3H)	1.34	OCH_2	1.26	OCH_2	1.29	OCH_2
$OCH_2C\underline{H}_3$ (3H)	1.18	OCH_2	1.18	OCH_2	1.21	OCH_2
$ArCH_3$ (3H)	–		2.22	Hb′	2.18	Hb′, Ha′

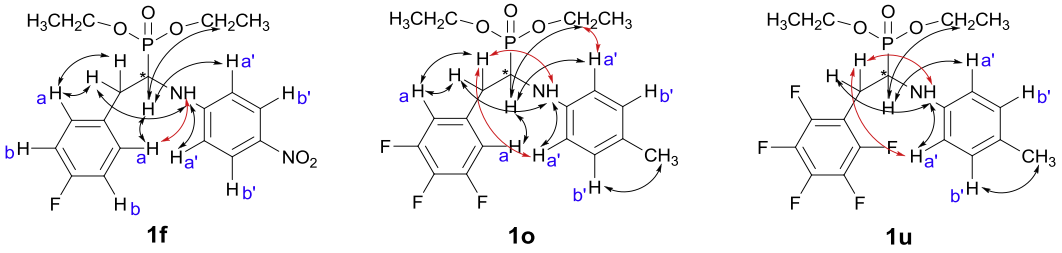

Fig. 7 Correlations observed in the NOESY spectra of **1f**, **1o** and **1u**. Correlations that are not envisioned in the all three spectra are presented in red.

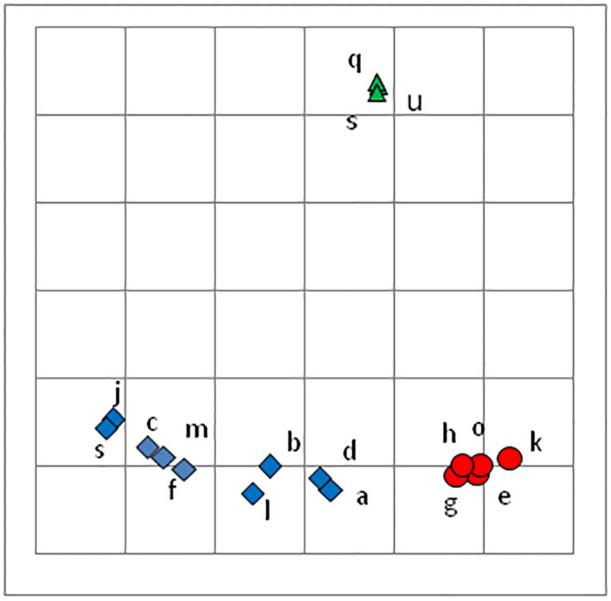

Fig. 8 Graphical 2D representation of 3-medoid clustering of crystal structures of the studied compounds.

mation B, and molecules {**1q**, **1s**, **1u**} in conformation C. Taking into account results of X-ray analysis, molecular structures of **1f**, **1o** and **1u** were selected as the representative conformations A, B, and C, respectively.

Table 5 presents the energy differences of these conformers calculated at wB97XD/6-311 + + G(d,p), B3LYP/6-311 + + G(d,p) and M06/6-311 + + G(d,p) levels for molecules **1f**, **1o** and **1u** *in vacuo*, and using the PCM model to take into account the effect of chloroform solution as NMR data were collected in $CDCl_3$ solvent. The energy differences between the three conformers observed in crystals are relatively small – not greater than 2.5 kcal/mol. Results of calculations performed with the functionals wB97XD and M06 in both *in vacuo*, as well as using the PCM indicated the conformation B as the one of the lowest energy. This conformation was found to be energetically preferable also on the basis of calculations performed using the B3LYP functional for the molecules *in vacuo*. Studies with this functional carried out with using the PCM showed that conformation B is characterized by the lowest energy for **1o** and **1u**, while for **1f** conformations A and B are almost equally favorable. In general the results obtained suggest that both isolated molecules as well as molecules in chloroform favor the B conformation, and the A and C conformations observed in crystals are likely the result of the intermolecular interactions (crystal packing).

Bond lengths calculated for conformers A, B, C, for **1f**, **1o** and **1u** at wB97XD/6-311 + + G(d,p), B3LYP/6-311 + + G(d,p) and M06/6-311 + + G(d,p) levels using the PCM model, and derived from X-ray studies are presented in Table S9 (ESI, page 200).

4. Conclusions

We synthesized a series of novel phosphonate analogues of phenylalanine containing variable number of fluorine substituents in different positions of the phenyl ring (**1a-u**), and subjected these compounds to structural studies by the use of both experimental and computational methods.

For 17 α-aminophosphonates crystal structures were determined. Single-crystal X-ray diffraction analysis revealed that the molecules investigated can adopt one of the three conformations A, B or C that are characterized by a set of torsion angles and dihedral angle defined between the planes of two aromatic rings. Conformer A is described by *ac-sc* combination of torsion angles and the dihedral angle of 45–83°, whereas in Conformer B and C the torsion angles combination is *ap-sc* and the aromatic rings are almost perpendicular to each other in conformer B, and are roughly parallel in conformer C. Interestingly, A is most commonly observed conformer in the crystals investigated; it occurs in 10 out of 17 crystal structures, while conformers B and C are present only in 5 and 3 crystal structures, respectively. This observation can suggest conformation A as most favorable in the solid state. On the other hand, results obtained from computational investigations performed at 6-311 + + G(d,p) basis set in all the DFT functionals used indicate that for the isolated molecules of all studied compounds conformation B is energetically favorable. However, the energy differences between the conformers A, B and C are not large (less than 3 kcal/mol), and preference for conformation A observed in crystal structures most likely results from intermolecular interactions.

The studied α-aminophosphonates have a big potential for biological activity and synthetic application. Formation of cyclic by-products by intramolecular nucleophilic aromatic substitution of initially obtained acyclic α-aminophosphonates shows that the later compounds may give access to even larger library of new potentially active molecules.

Table 5 Relative energies in [kcal/mol] of conformers A, B, and C for molecules **1f**, **1o**, and **1u**.

Molecule	Conf.	wB97XD/6-311 + + G(d,p)		B3LYP/6-311 + + G(d,p)		M06/6-311 + + G(d,p)	
		In vacuo	In chloroform	*In vacuo*	In chloroform	*In vacuo*	In chloroform
1f	A	1.36	0.91	0.33	0.00	0.49	0.09
1f	B	0.00	0.00	0.00	0.02	0.00	0.00
1f	C	0.99	1.52	1.81	2.31	0.99	1.50
1o	A	2.41	1.93	1.41	1.01	1.47	1.10
1o	B	0.00	0.00	0.00	0.00	0.00	0.00
1o	C	0.57	1.19	1.40	1.96	0.59	1.19
1u	A	1.38	1.37	0.92	0.80	0.71	0.76
1u	B	0.00	0.00	0.00	0.00	0.00	0.00
1u	C	0.34	0.82	1.41	1.85	1.04	1.85

Acknowledgements

This research was supported in part by PL-Grid Infrastructure (http://www.plgrid.pl/en).

Declaration of interest

The authors declare no conflicts of interests.

Appendix A. Supplementary material

Supplementary data associated with this article can be found, in the online version, at https://doi.org/10.1016/j.arabjc.2018.05.002.

Notes

CCDC 1562711-1562727 contain the supplementary crystallographic data for this paper. These data can be obtained free of charge from The Cambridge Crystallographic Data Centre via www.ccdc.cam.ac.uk/data%5Frequest/cif.

References

Abdi, H., Williams, L.J., 2010. Principal component analysis. Wiley Interdiscip. Rev. Comput. Stat. 2, 433–459. https://doi.org/10.1002/wics.101.

Ajenjo, J., Greenhall, M., Zarantonello, C., Beier, P., 2016. Synthesis and nucleophilic aromatic substitution of 3-fluoro-5-nitro-1-(pentafluorosulfanyl)benzene. Beilstein J. Org. Chem. 12, 192–197. https://doi.org/10.3762/bjoc.12.21.

Atherton, F.R., Hassall, C.H., Lambert, R.W., 1986. Synthesis and structure-activity relationships of antibacterial phosphonopeptides incorporating (1-aminoethyl)phosphonic acid and (aminomethyl) phosphonic acid. J. Med. Chem. 29, 29–40.

Barbour, L.J., 2001. X-seed—a software tool for supramolecular crystallography. J. Supramol. Chem. 1, 189–191. https://doi.org/10.1016/S1472-7862(02)00030-8.

Bartlett, P.A., Hunt, J.T., Adams, J.L., Gehret, J.-C.E., 1978. Phosphorus-containing purines and pyrimidines: a new class of transition state analogs. Bioorganic Chem. 7, 421–436. https://doi.org/10.1016/0045-2068(78)90033-0.

Becke, A.D., 1993. Density-functional thermochemistry. III. The role of exact exchange. J. Chem. Phys. 98, 5648–5652. https://doi.org/10.1063/1.464913.

Bernhard, S.A., Orgel, L.E., 1959. Mechanism of enzyme inhibition by phosphate esters. Science 130, 625–626. https://doi.org/10.1126/science.130.3376.625.

Bruno, I.J., Cole, J.C., Edgington, P.R., Kessler, M., Macrae, C.F., McCabe, P., Pearson, J., Taylor, R., 2002. New software for searching the Cambridge Structural Database and visualizing crystal structures. Acta Crystallogr. B 58, 389–397.

Chai, J.-D., Head-Gordon, M., 2008. Long-range corrected hybrid density functionals with damped atom–atom dispersion corrections. Phys. Chem. Chem. Phys. 10, 6615–6620. https://doi.org/10.1039/B810189B.

Cherkasov, R.A., Galkin, V.I., 1998. The Kabachnik-Fields reaction: synthetic potential and the problem of the mechanism. Russ. Chem. Rev. 67, 857–882. https://doi.org/10.1070/RC1998v067n10ABEH000421.

Clark, T., Chandrasekhar, J., Spitznagel, G.W., Schleyer, P.V.R., 1983. Efficient diffuse function-augmented basis sets for anion calculations. III. The 3–21 + G basis set for first-row elements, Li–F. J. Comput. Chem. 4, 294–301. https://doi.org/10.1002/jcc.540040303.

Cobb, S.L., Murphy, C.D., 2009. 19F NMR applications in chemical biology. J. Fluor. Chem. 130, 132–143. https://doi.org/10.1016/j.jfluchem.2008.11.003.

CrysAlisPro, version 171.38.46, 2015. Agilent Technologies, Ltd, Yarnton, England.

Desiraju, G.R., Steiner, T., 1999. The Weak Hydrogen Bond in Structural Chemistry and Biology. OUP, Chichestre.

Francl, M.M., Pietro, W.J., Hehre, W.J., Binkley, J.S., Gordon, M.S., DeFrees, D.J., Pople, J.A., 1982. Self-consistent molecular orbital methods. XXIII. A polarization-type basis set for second-row elements. J. Chem. Phys. 77, 3654–3665. https://doi.org/10.1063/1.444267.

Gillis, E.P., Eastman, K.J., Hill, M.D., Donnelly, D.J., Meanwell, N. A., 2015. Applications of fluorine in medicinal chemistry. J. Med. Chem. 58, 8315–8359. https://doi.org/10.1021/acs.jmedchem.5b00258.

Gutsche, C.S., Ortwerth, M., Gräfe, S., Flanagan, K.J., Senge, M.O., Reissig, H.-U., Kulak, N., Wiehe, A., 2016. Nucleophilic aromatic substitution on pentafluorophenyl-substituted dipyrranes and tetrapyrroles as a route to multifunctionalized chromophores for potential application in photodynamic therapy. Chem. - Eur. J. 22, 13953–13964. https://doi.org/10.1002/chem.201601857.

Hariharan, P.C., Pople, J.A., 1973. The influence of polarization functions on molecular orbital hydrogenation energies. Theor. Chim. Acta 28, 213–222. https://doi.org/10.1007/BF00533485.

Huang, X.-C., Wang, M., Pan, Y.-M., Yao, G.-Y., Wang, H.-S., Tian, X.-Y., Qin, J.-K., Zhang, Y., 2013. Synthesis and antitumor activities of novel thiourea α-aminophosphonates from dehydroabietic acid. Eur. J. Med. Chem. 69, 508–520. https://doi.org/10.1016/j.ejmech.2013.08.055.

Jang, M.-Y., Lin, Y., De Jonghe, S., Gao, L.-J., Vanderhoydonck, B., Froeyen, M., Rozenski, J., Herman, J., Louat, T., Van Belle, K., Waer, M., Herdewijn, P., 2011. Discovery of 7-*N*-Piperazinylthiazolo[5,4- *d*]pyrimidine analogues as a novel class of immunosuppressive agents with in vivo biological activity. J. Med. Chem. 54, 655–668. https://doi.org/10.1021/jm101254z.

Kafarski, P., Lejczak, B., 1991. Biological activity of aminophosphonic acids. Phosphorus Sulfur Silicon Relat. Elem. 63, 193–215. https://doi.org/10.1080/10426509108029443.

Kawasaki, M., Goto, M., Kawabata, S., Kometani, T., 2001. The effect of vinyl esters on the enantioselectivity of the lipase-catalysed transesterification of alcohols. Tetrahedron Asymm. 12, 585–596. https://doi.org/10.1016/S0957-4166(01)00083-0.

Khatri, C.K., Satalkar, V.B., Chaturbhuj, G.U., 2017. Sulfated polyborate catalyzed Kabachnik-fields reaction: an efficient and eco-friendly protocol for synthesis of α-amino phosphonates. Tetrahedron Lett. 58, 694–698. https://doi.org/10.1016/j.tetlet.2017.01.022.

Kolonko, K.J., Reich, H.J., 2008. Stabilization of ketone and aldehyde enols by formation of hydrogen bonds to phosphazene enolates and their aldol products. J. Am. Chem. Soc. 130, 9668–9669. https://doi.org/10.1021/ja804221x.

Korb, M., Swarts, P.J., Miesel, D., Hildebrandt, A., Swarts, J.C., Lang, H., 2016. Nucleophilic aromatic substitution reactions for the synthesis of ferrocenyl aryl ethers. Organometallics 35, 1287–1300. https://doi.org/10.1021/acs.organomet.6b00157.

Krishnan, R., Binkley, J.S., Seeger, R., Pople, J.A., 1980. Self-consistent molecular orbital methods. XX. A basis set for correlated wave functions. J. Chem. Phys. 72, 650–654. https://doi.org/10.1063/1.438955.

Kukhar, V.P., Hudson, H.R., 2000. Aminophosphonic and Aminophosphinic Acids: Chemistry and Biological Activity.

Lee, C., Yang, W., Parr, R.G., 1988. Development of the Colle-Salvetti correlation-energy formula into a functional of the electron density. Phys. Rev. B 37, 785–789. https://doi.org/10.1103/PhysRevB.37.785.

Lejczak, B., Kafarski, P., Zygmunt, J., 1989. Inhibition of aminopeptidases by aminophosphonates. Biochemistry (Mosc.) 28, 3549–3555.

Li, Y.-J., Wang, C.-Y., Ye, M.-Y., Yao, G.-Y., Wang, H.-S., 2015. Novel coumarin-containing aminophosphonatesas antitumor agent: synthesis, cytotoxicity, DNA-binding and apoptosis evaluation. Molecules 20, 14791–14809. https://doi.org/10.3390/molecules200814791.

Lombaert, S.D., Blanchard, L., Tan, J., Sakane, Y., Berry, C., Ghai, R.D., 1995. Non-peptidic inhibitors of neutral endopeptidase 24.11 1. Discovery and optimization of potency. Bioorg. Med. Chem. Lett. 5, 145–150. https://doi.org/10.1016/0960-894X(94)00474-T.

Makhaeva, G.F., Aksinenko, A.Y., Sokolov, V.B., Baskin, I.I., Palyulin, V.A., Zefirov, N.S., Hein, N.D., Kampf, J.W., Wijeyesakere, S.J., Richardson, R.J., 2010. Kinetics and mechanism of inhibition of serine esterases by fluorinated aminophosphonates. Chem. Biol. Interact. 187, 177–184. https://doi.org/10.1016/j.cbi.2009.12.018.

Møller, C., Plesset, M.S., 1934. Note on an approximation treatment for many-electron systems. Phys. Rev. 46, 618–622. https://doi.org/10.1103/PhysRev. 46.618.

Mucha, A., Kafarski, P., Berlicki, Ł., 2011. Remarkable potential of the α-aminophosphonate/phosphinate structural motif in medicinal chemistry. J. Med. Chem. 54, 5955–5980. https://doi.org/10.1021/jm200587f.

Park, H.-S., Jun, C.-H., 2009. A simple and fast algorithm for K-medoids clustering. Expert Syst. Appl. 36, 3336–3341. https://doi.org/10.1016/j.eswa.2008.01.039.

POV-RayTM for Windows, version 3.6, Persistence of Vision Raytracer Pty Ltd, 2004. Williamstown, Australia.

Rao, Y.S., Filler, R., 1974. Novel method for the oxidation of primary and secondary alcohols to carbonyl compounds. J. Org. Chem. 39, 3304–3305. https://doi.org/10.1021/jo00936a040.

Reddy, B.V.S., Krishna, A.S., Ganesh, A.V., Kumar, G.G.K.S.N., 2011. Nano Fe3O4 as magnetically recyclable catalyst for the synthesis of α-aminophosphonates in solvent-free conditions. Tetrahedron Lett. 52, 1359–1362. https://doi.org/10.1016/j.tetlet.2011.01.074.

Rezaei, Z., Firouzabadi, H., Iranpoor, N., Ghaderi, A., Jafari, M.R., Jafari, A.A., Zare, H.R., 2009. Design and one-pot synthesis of α-aminophosphonates and bis(α-aminophosphonates) by iron(III) chloride and cytotoxic activity. Eur. J. Med. Chem. 44, 4266–4275. https://doi.org/10.1016/j.ejmech.2009.07.009.

Sheldrick, G.M., 2015. Crystal structure refinement with SHELXL. Acta Crystallogr. Sect. C Struct. Chem. 71, 3–8. https://doi.org/10.1107/S2053229614024218.

Smart, B.E., 2001. Fluorine substituent effects (on bioactivity). J. Fluor. Chem. 109, 3–11. https://doi.org/10.1016/S0022-1139(01)00375-X.

Song, B.-A., Wu, Y.-L., Yang, S., Hu, D.-Y., He, X.-Q., Jin, L.-H., 2003. Synthesis and bioactivity of a-aminophosphonates containing fluorine. Molecules 8, 186–192. https://doi.org/10.3390/80100186.

Szekely, G.J., Rizzo, M.L., 2005. Hierarchical clustering via joint between-within distances: extending Ward's minimum variance method. J. Classif. 22, 151–183. https://doi.org/10.1007/s00357-005-0012-9.

Wang, Q., Yang, L., Ding, H., Chen, X., Wang, H., Tang, X., 2016. Synthesis, X-ray crystal structure, DNA/protein binding and cytotoxicity studies of five α-aminophosphonate N-derivatives. Bioorganic Chem. 69, 132–139. https://doi.org/10.1016/j.bioorg.2016.10.007.

Wang, Q., Zhu, M., Zhu, R., Lu, L., Yuan, C., Xing, S., Fu, X., Mei, Y., Hang, Q., 2012. Exploration of α-aminophosphonate N-derivatives as novel, potent and selective inhibitors of protein tyrosine phosphatases. Eur. J. Med. Chem. 49, 354–364. https://doi.org/10.1016/j.ejmech.2012.01.038.

Wolff, S.K., Grimwood, D.J., McKinnon, J.J., Turner, M.J., Jayatilaka, D., Spackman, M.A., 2013. Crystal Explorer ver. 3.1. Perth, University of Western Australia.

Yang, S., Gao, X.-W., Diao, C.-L., Song, B.-A., Jin, L.-H., Xu, G.-F., Zhang, G.-P., Wang, W., Hu, D.-Y., Xue, W., Zhou, X., Lu, P., 2006. Synthesis and antifungal activity of novel chiralα-aminophosphonates containing fluorine moiety. Chin. J. Chem. 24, 1581–1588. https://doi.org/10.1002/cjoc.200690296.

Zhao, Y., Truhlar, D.G., 2008. The M06 suite of density functionals for main group thermochemistry, thermochemical kinetics, noncovalent interactions, excited states, and transition elements: two new functionals and systematic testing of four M06-class functionals and 12 other functionals. Theor. Chem. Acc. 120, 215–241. https://doi.org/10.1007/s00214-007-0310-x.